Construction and Building Materials 315 (2022) 125640

Contents lists available at ScienceDirect

Construction and Building Materials

journal homepage: www.elsevier.com/locate/conbuildmat

Thermal mortar-based insulation solutions for historic walls: An extensive hygrothermal characterization of materials and systems

Magda Posani [a,b,*], Rosário Veiga [a], Vasco Peixoto de Freitas [b]

[a] Buildings Department, LNEC – National Laboratory for Civil Engineering, Av. Do Brasil 101, 1700-066 Lisboa, Portugal
[b] CONSTRUCT (LFC—Laboratory of Building Physics), Faculty of Engineering (FEUP), University of Porto, Rua Doutor Roberto Frias, s/n, 4200-465 Porto, Portugal

ARTICLE INFO

Keywords:
Hygric properties
Thermal properties
Hygrothermal characterization
Thermal mortars
Thermal conductivity
Sorption isotherm
Water vapour diffusion
Capillary water absorption
WUFI data

ABSTRACT

Among thermal insulation solutions for historic walls, thermal renders and plasters appear to be a very feasible option. Thus, this work analyses commercially available thermal mortars suitable for the scope.

An extensive experimental campaign showed that testing single materials only, which is the standard requirement for thermal mortar-based systems, is in fact not sufficient for understanding the potential impact of the intervention on walls: whole-systems should also be examined. This study provides a detailedcharacterization of materials and systems, useful as a database for forthcoming investigations on compatibility and efficacy for application on historic walls, via numerical hygrothermal simulations.

1. Introduction

Climate change has become so serious that it is believed to be one of the defining issues of the current century [1,2]. For this reason, the European Union is pursuing an ambitious policy on climate actions, urgently calling for an acceleration in the transition towards net-zero emissions [3]. In this scenario, the strategic importance of energy-efficient renovations in the existing building stock is evident [4,5], and increasing attention has been paid to the specific context of historic constructions [6–9]. Furthermore, retrofits of historic buildings not only offer the chance to reduce their carbon footprints, but also improve their preservation and durability. Indeed, energy-efficient interventions can enhance indoor comfort [10] while lowering operational costs [11]. These two factors are fundamental in ensuring the continued use of historic buildings over time, which in turn leads to regular maintenance and better preservation of the constructions [12], in accordance with integrated conservation strategies [13].

One of the energy-efficient interventions discussed in the literature consists of improving the thermal resistance of historic walls by means of thermal insulation solutions [14]. For this purpose, thermal mortars represent a very feasible option for several reasons. They are typically easy to remove [15], which is important for the reversibility of the intervention [16], and they require no anchoring points [17]. They offer great flexibility for the thickness, which can be easily adapted to the dimensional restriction required in the intervention [18]. Furthermore, thermal mortars guarantee adaptability to uneven surfaces and gap-filling ability [19], thus allowing for continuous contact between the insulation layer and the substrate even in the case of irregularities, cracks and other damages which are quite commonly found in historic components.

The nomenclature “thermal mortar” indicates a mortar with thermal insulation properties, namely a thermal conductivity lower than 0.2 W/(m.K) at 10 °C, according to standard EN 998-1:2017 [20]. Thermal mortars can be applied to the external or internal side of building components, and they may be referred to as thermal renders [21] or thermal plasters [22], respectively in the former and latter cases. Thermal mortars are generally obtained using lightweight aggregates in the mix design. For instance, several studies have considered mortars with Expanded Polystyrene (EPS) and/or cork aggregates [23 –26], while other investigations have analysed the thermal benefits provided by the addition of hemp [27], expanded clay [28], silica aerogel [29,30], expanded glass and perlite [31]. Additionally, some authors have accounted for the environmentally-friendly nature of reusing waste in building materials [32,33] by incorporating olive stones [34] and plastic waste [35] in energy-efficient mortars. In the context of heritage buildings, Walker and Pavia [36] adopted lime plasters containing cork

* Corresponding author at: Buildings Department, LNEC – National Laboratory for Civil Engineering, Av. Do Brasil 101, 1700-066 Lisboa, Portugal.
E-mail address: mposani@lnec.pt (M. Posani).

https://doi.org/10.1016/j.conbuildmat.2021.125640
Received 4 June 2021; Received in revised form 25 September 2021; Accepted 8 November 2021
Available online 6 December 2021

and hemp in a field investigation on historic walls, while other authors have analysed the use of mortars containing aerogel [17], expanded glass [37] and perlite [38,39]. Thermal mortars have also been considered in several studies investigating thermal retrofit solutions for historic buildings via numerical simulations [40–45].

This work takes into analysis a set of thermal insulation solutions based on thermal mortars which are commercially available and designed for interventions on historic or masonry/stone walls. The experimental campaign investigates the hygrothermal behaviour of single materials and whole insulation systems. The properties considered are open porosity, dry bulk density, thermal conductivity (dry and moisture-dependent), specific heat capacity, sorption isotherm, resistance to water vapour diffusion (via dry and wet-cup) and capillary water absorption coefficient. Testing procedures and samples characteristics are defined following two regulations: the European specifications for mortars for masonry – EN 998-1:2017 [20] and the Guideline for European technical approval of External Thermal Insulation Composite Systems (ETICS) with rendering – ETAG 004 [46]. The first standard sets the requirements for commercial mortars in Europe and it is the one adopted by manufacturers to certify and classify thermal mortar-based insulation systems. This standard accounts for tests on samples of single or painted materials. ETAG 004 is the guideline adopted to certify (CE marking) other types of composite insulation systems that are not covered by harmonized European standards, namely ETICS. ETAG 004 accounts for samples of complete multi-layered systems. The results obtained with standard samples of single materials and composite samples of complete systems are compared and discussed. This analysis aims to evaluate whether and how the layered structure of the systems and the presence of inter-layer interfaces affects the performance of composite insulation solutions based on thermal mortars.

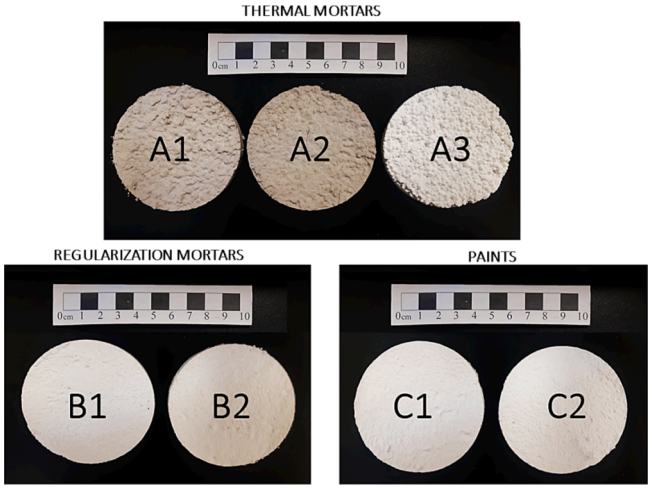

Fig. 1. Materials considered in the study. Two thermal mortars with hydraulic lime and cork-aggregates (A1, A2), and one with mixed binders and EPS-aggregates (A3). Two regularization mortars, one based on air lime (B1) and one based on mixed hydraulic binders (B2). A lime-paint (C1) and a potassium silicate paint (C2).

Overall, this study has the following goals:

- providing an exhaustive hygrothermal characterization of the selected materials and systems, useful as a database for forthcoming investigations on compatibility and efficacy for application on historic walls, via numerical hygrothermal simulations;
- discussing the appropriateness of standard EN 998-1:2017 for the characterization of insulation solutions based on thermal mortars, considering that it neglects the behaviour of complete insulation systems as whole units.

2. Materials

This study investigates thermal insulation systems based on thermal mortars which are commercially available and designed for application

Table 1
Materials and systems considered in the study. Manufacturers' declared values of vapour resistance factor and capillary water absorption coefficients of the materials, and the declared thermal conductivity of thermal mortars. The missing values are not declared in technical sheets or disregarded.

Producer	Identification	Code	μ [-] *Declared vapour resistance factor	A_w [kg/(m^{2}min$^{0.5}$)] *Declared capillary water absorption coefficient	λ [W/(mK)] *Declared Thermal conductivity
			Materials (main binders and lightweight aggregates)		
1st	Thermal mortar 1 (Hydraulic lime and Cork aggregates)	A1	4	0.4	0.045
	Thermal mortar 2 (Hydraulic lime and Cork aggregates)	A2	4	0.63	0.08
	Regularization Mortar (Air lime)	B1	≤ 15	≥0.40	/
	Paint (Lime-based) – Indoor use	C1	*"breathable"*	/	/
	Paint (Potassium silicate-based) – Outdoor use	C2	*"breathable"*	*"Water-repellent"*	/
2nd	Thermal mortar 3 (Mixed binders and EPS aggregates)	A3	≤ 5	≤ 0.2	0.05
	Regularization and finishing Mortar (Mixed Hydraulic binders)	B2	≤ 5	≤ 0.2	/

**All properties reported in the technical sheets of thermal mortars were determined according to the indications of EN998-1 [20] (i.e. test methods referred in standards EN 1015–19 [49], EN 1015–18 [53], EN 1745 [54] for μ, A_w and λ). For thermal mortar A3, the manufacturer further specifies the additional use of standard EN 12664 [96], which is the one designated by EN1745 for tests involving guarded hot plates and heat flow meters.*

	Systems	
1st	S1: A1 + B1 + C1 (Indoor use)	S1
	S2: A1 + B1 + C2 (Outdoor use)	S2
	S3: A2 + B1 + C1 (Indoor use)	S3
	S4: A2 + B1 + C2 (Outdoor use)	S4
2nd	S5: A3 + B2 (Indoor and outdoor use)	S5

on historic or traditional masonry walls. The three thermal mortars considered can be described as having low water absorption coefficients and high vapour permeability, according to the classification proposed in a previous study on the compatibility of thermal insulations for historic buildings [47] (manufacturers' declared properties:

$A_w < 0.11$ kg $m^{-2}s^{-1/2}$, $\delta_p \geq 17.9\ 10^{-12}$ kg m^{-1} s^{-1} Pa^{-1}). Their declared values of thermal conductivity are in the range of 0.045–0.08 W/(m.K), and they are developed by two different manufacturers. From the first manufacturer, two lime-cork mortars (A1, A2) are analysed. These materials are designed to be covered with a regularization mortar (B1) and a final layer of paint: a lime-based one (C1) for indoor-exposed systems and one with potassium silicate (C2) for external solutions, both of which are declared to be "breathable" finishings. Hence, 4 systems (S1, S2, S3, S4) are considered from the first manufacturer: two based on the first thermal mortar (S1: A1 + B1 + C1, S2: A1 + B1 + C2) and two on the second one (S3: A2 + B1 + C1, S4: A2 + B1 + C2). From the second producer, a mortar based on mixed binders and Expanded Polystyrene (EPS) aggregates is considered (A3). This material is used in combination with a regularization mortar that also works as a finishing layer (B2) and the system (S5) is suitable for both interior and exterior interventions (S5: A3 + B2).All in all, 7 materials and 5 systems are tested, as shown in Fig. 1 and Table 1.

3. Methods

For each type of sample, three specimens were prepared and tested for the sake of taking potential irregularities into account [39]. Test results are expressed as the average of the measurements performed on the three specimens, and an estimation of the error is provided by using the Standard Error of the Mean (SEM, with 2 significative digits), i.e. the standard deviation (σ) divided by the square root of the number of measurements ($SEM = \sigma/\sqrt[2]{3}$).

3.1. Samples preparation and geometry

To assess the hygrothermal properties of hardened materials and systems, different types of specimens were considered. The characteristics of the samples and the properties tested are summarized in Table 2, while the moulds adopted are shown in Fig. 2. The first three types (a, b, c in Fig. 2) were used to prepare standard samples aligned with EN 998-1 by pouring in fresh mortars, storing them in a conditioned room (23 °C ± 5 °C, 50% ± 5% RH), and demoulding after 5 days. The samples were left in the same conditions for a further 85 days, reaching a 90-day curing time. After that, some samples were finished with paint and left to dry under the same controlled conditions for 15 days more. The last type of mould, (d in Fig. 2), was used to prepare thicker tile samples that better represent real applications, following the indications of ETAG 004. In these moulds, large tiles (550 mm x150mm x40mm) of thermal mortars were prepared with two successive layers, each one 20 mm thick, as required in the materials technical sheets. In further detail, the first layer of mortar was poured and left for 24 h at "normal indoor conditions" (free-floating indoor microclimate, 13–20 °C and 40–80% RH were registered). Then, the mortar surface was moistened, and a new layer of fresh material was applied. After 5 days of drying under "normal indoor conditions", the hardened samples were demoulded, and they were put under controlled conditions (23 °C ± 5 °C; 50% ± 5% RH) until reaching a 90-day curing period. Thereafter, the tiles were cut into smaller specimens. Some of these smaller samples were covered with a layer of regularization mortar and left to cure at controlled conditions for a further month. Part of them were then finished with paint and put to dry under controlled conditions for 15 days more. The tile samples of thermal mortars created with this method have a thickness of about 40 mm, while the ones to which also regularization mortar was applied, with or without paint, have an average thickness of 42 mm.

The timing adopted for curing and demoulding the samples was chosen for several reasons. A period of 5 days was adopted for the demoulding to comply with the minimum time prescribed by standard EN 1015–11:2019 [48], i.e. 2 to 5 days depending on the binder. Thus, the maximum time was adopted for all mortars to homogenize demoulding schedules, while avoiding the risk of mortars with longer setting times breaking in the process. A 90-day curing time was chosen to allow the specimens of mortars to reach a high level of carbonation, while complying with the minimum reference time referred to in norm 1015–19 (28 days) [49]. Moreover, 90 days is a curing period often adopted for testing lime-based materials [50,51]. A curing period of 30 days was selected for the regularization layer applied on tiles of thermal mortars to comply with the minimum time period of standard 1015–19. It was considered sufficient for carbonation because of the very reduced thickness of this layer (about 2 mm). A curing time of 15 days was defined for the paints applied on samples to comply with the minimum time required in standard EN1062-3 [52] for finishings (7 days).

3.2. Test procedures

The methods and standards adopted for the experimental campaign are presented in Table 3 and they are described in detail in the following sections. The main European standard for product qualification of thermal mortars, and all mortars in general, is EN 998-1:2017 [20]. It provides some indications concerning the classification of the materials, based on their physical, mechanical and hygrothermal properties, as well as other characteristics such as fire resistance and durability. Moreover, it indicates minimum performance requirements and reference standards for testing procedures. In terms of hygrothermal properties, standard EN 998-1 accounts for capillary water absorption, resistance to water vapour diffusion and thermal conductivity, recommending standards EN1015-18 [53], EN1015-19 [49] and EN1745 [54] for the corresponding test methods. Commercial thermal mortar-based systems are required to comply with the indications of standard EN 998-1 for single materials. On the contrary, other insulation solutions, such as ETICS (External Thermal Insulation Composite Systems), must comply with the requirements defined by the European Guidelines ETAG 004 [46]. This last standard accounts for tests performed on samples of complete insulation solutions, thus considering the behaviour of each system as a whole. In this work, both regulations are accounted for in the test procedures. Standard samples of single and painted materials are tested with consideration of the European specifications EN 998-1, while tile samples of single and combined materials, as well as complete systems, are evaluated accounting for the indications of ETAG 004.

In regards to capillary water absorption and resistance to water vapour diffusion, the European Committee for Standardization (CEN) also provides some specifications for testing materials for interventions on heritage buildings: standards EN15801:2009 [57] and EN15803:2009 [59]. These two regulations are thus taken into account in the testing procedures and in the analysis of results. Concerning dry bulk density, even though standard EN 998-1 recommends adopting a test of full immersion in water as in EN1015-10 [60], the testing procedure FE Pa 44 [55] is hereby preferred because it defines the measurement of both dry bulk density and open porosity, by means of the same test of immersion in water under vacuum conditions. Standard 998-1 and Guidelines ETAG 004 do not consider properties related to the hygroscopic behaviour of materials and systems, such as the sorption isotherm. For this reason, the international standard ISO 12571 [56] is adopted. Finally, thermal properties are measured with a Modified Transient Plane Source (MTPS). Hence, in addition to standard EN1745, also ASTM D7984:2016 [58] is considered since it specifically addresses the use of MTPS equipment.

3.2.1. Open porosity and dry bulk density

The dry bulk density and open porosity of hardened mortars were determined using the testing procedure FE Pa 44 – "Determination of

Table 2
Summary of the specimens adopted.

Samples	Size	Material	Properties tested
Standard samples: single materials and applied paints. Based on EN 998-1:2017			
Prism	160 mm × 40 mm × 40 mm	A1-Thermal mortar A2 - Thermal mortar B1- Regularization mortar A3 - Thermal mortar B2- Regularization mortar	Dry bulk density and open porosity Capillary water absorption
Disk	ϕ 200 mm × 20 mm	A1 - Thermal mortar A2 - Thermal mortar B1- Regularization mortar B1 + C1- Reg. m + Finishing 1 B1 + C2- Reg. m. + Finishing 2 A3 - Thermal mortar B2- Regularization mortar	Resistance to water vapour diffusion
Small disk	ϕ 70 mm × 10 mm	A1 - Thermal mortar A2 - Thermal mortar B1- Regularization mortar B1 + C1- Reg. m. + Finishing 1 B1 + C2- Reg. m. + Finishing 2 A3 - Thermal mortar B2- Regularization mortar	Sorption isotherm
Tile samples: thermal mortars, addition of regularization layer, and complete systems. Samples prepared by layers to better represent real applications, based on ETAG 004 guidelines for composite insulation systems.			
Tile*	150 mm × 150 mm × *40 mm	A1 A1 + B1 S1 (=A1 + B1 + C1) S2 (=A1 + B1 + C2) A2 A2 + B1 S3 (=A2 + B1 + C1) S4 (=A2 + B1 + C2) A3 S5 (=A3 + B2)	Capillary water absorption
Tile*	110 mm × 150 mm × *40 mm	A1 A1 + B1 S1 (=A1 + B1 + C1) S2 (=A1 + B1 + C2) A2 A2 + B1 S3 (=A2 + B1 + C1) S4 (=A2 + B1 + C2) A3 S5 (=A3 + B2)	Resistance to water vapour diffusion
Tile*	90 mm × 50 mm × *40 mm	S1 (=A1 + B1 + C1) S2 (=A1 + B1 + C2) S3 (=A2 + B1 + C1) S4 (=A2 + B1 + C2) S5 (=A3 + B2)	Sorption isotherm
Tile	150 mm × 150 mm × 40 mm	A1, A2, A3	Thermal conductivity Specific heat capacity

*In these samples, 40 mm thickness refers to the layer of thermal mortar. The average thickness of samples where regularization mortars B1 or B2 were applied, with and without paint, is on average 42 mm.

open porosity and bulk and real densities" [55]. For each hardened mortar, three prism specimens (160 × 40 × 40 mm) were cut into two halves and only one of them was tested. The specimens were dried to constant mass (M_{dry}) in a ventilated oven (40 ± 5 °C) and then put under vacuum conditions for 24 h (±2h) in a desiccator (400 mbar, Fig. 3a). The desiccator was then filled with distilled water to keep the specimens full-immersed, under vacuum conditions, for a further 24 h (±2h). The samples were then removed from the desiccator and their mass was measured via hydrostatic (M_h) and gravimetric (M_{sat}) weighing. Open porosity (P_o) and dry bulk density (ρ_{dry}) were then defined according to Eqs. (1) and (2):

$$P_O = \frac{M_{sat} - M_{dry}}{\rho_w} \cdot \frac{1}{V} \cdot 100\% = \frac{M_{sat} - M_{dry}}{M_{sat} - M_h} \cdot 100\% \quad (1)$$

$$\rho_{dry} = \frac{M_{dry}}{V} \quad (2)$$

3.2.2. Thermal conductivity and specific heat capacity

Measurements of thermal conductivity in building materials may be performed through a variety of methods, which are broadly classified into two categories: steady-state methods and transient methods [61]. A transient method was chosen in this study (Modified Transient Plane Source, MTPS), because of the several benefits it offers [27,62,63]. Transient methods measure both thermal conductivity and specific heat capacity within the same test. Moreover, they require smaller samples, their results depend less on the operator, they are more appropriate for measurements on moist materials and easier to perform than the steady-state tests.

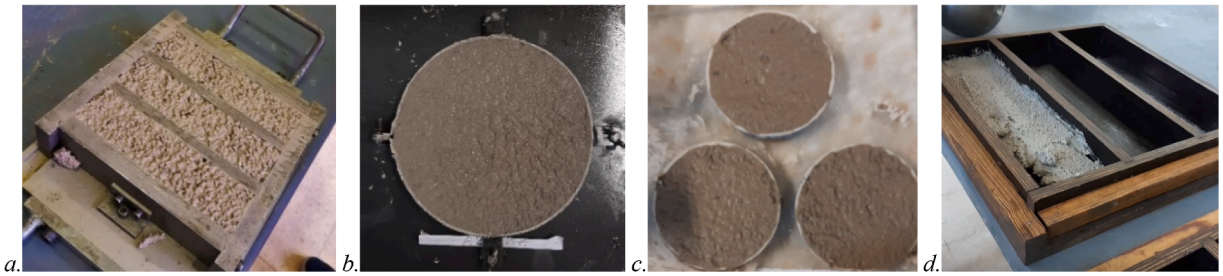

Fig. 2. Moulds used for (a) prism, (b) disk, (c) small disk and (d) tile samples.

Table 3
Summary of the test methods and standards adopted in the experimental campaign.

Samples	Property	Standards/Test procedures	Method
Tests on physical properties			
Standard samples	- Open porosity - Dry bulk density	FE Pa 44 [55]	Water saturation under vacuum conditions
Tests on hygric properties			
Standard samples	- Sorption isotherm	ISO 12571:2013 [56]	Climatic chamber
	- Resistance to water vapour diffusion	EN 1015–19 [49] EN 15803:2009 [59]	Dry-cup Wet-cup
	- Capillary water absorption	EN 1015–18:2002 [53] EN 15801:2009 [57]	One-direction absorption by partial immersion
Tile samples	- Sorption isotherm	ISO 12571:2013 [56]	Climatic chamber
	- Resistance to water vapour diffusion	ETAG 004 [46]	Dry-cup Wet-cup
	- Capillary water absorption	ETAG 004 [46]	One-direction absorption by partial immersion
Tests on thermal properties			
Tile samples of Thermal mortars	- Thermal conductivity ($\lambda_{10°C,dry}$) - Specific heat capacity (c_{dry}) - Thermal conductivity, moisture dependent (at 23 °C)	EN 1745 [54] ASTM D7984:2016 [58] Test procedure explained in the text	MTPS (Modified transient plane source)

Specimens of thermal mortars (150 × 150 × 40 mm) were tested with an ISOMET 2114 (MTPS, Applied Precision, Ltd), as shown in Fig. 3b, and the test was based on the indications of standards EN1745:2020 [54] and ASTM D7984:2016 [58]. The thermal conductivity and specific heat capacity of the samples were first determined at dry, standard conditions (10 °C) [54]. Then the thermal conductivity of moist samples was measured, which is a very important piece of information for evaluating their thermal performance at realistic in-situ conditions [64,65]. Specifically, the samples were soaked with liquid water, and then left to dry under controlled conditions (23 °C ± 5 °C, 50% ± 5% RH). During this time, their thermal conductivity was determined at three different moisture states, similar to in Parracha et Al.[66]. The water content of tested samples was defined as the average between the initial and final amounts during the MTPS measurement performed, while potential inhomogeneities in moisture distribution through the sample were disregarded. Thermal properties were measured only for thermal mortars because these are the only insulation materials adopted in the solutions considered, thus they are the ones whose properties determine the thermal performance of the systems.

3.2.3. Sorption isotherm

Porous materials exposed to constant conditions of temperature and relative humidity tend to exchange moisture with the environment until reaching a state of equilibrium [67]. The sorption isotherm describes the relationship between relative humidity and equilibrium moisture content of a material in the hygroscopic range [68], at a constant temperature. Sorption isotherms are necessary in analysing the moisture condition of structures [67], especially when multi-layered systems with no capillary-breaking separations are analysed, which is the case of mortars applied on masonry components [69].

The determination of moisture content in the hygroscopic range is based on the climatic chamber method defined in ISO 12571: 2013 [56]. All thermal mortars were tested, as well as the regularization mortars with and without the finishing paints (small disks in Fig. 3c) and samples of complete systems (tiles in Fig. 3c). The lateral surface and base of each sample were sealed, then the specimens were dried to constant mass (M_{dry}) and put in the climatic chamber, where the environment was kept at a constant Temperature (T) of 23 °C, while the Relative Humidity (RH) of the air was periodically increased through the following steps: 30%; 50%; 70%; 80% and 95%. The mass of the samples was weighed every 24 h until reaching the equilibrium state (mass M_{RH_i}) and the corresponding moisture content (w_{RH_i}) was obtained as:

$$w_{RH\_i} = \frac{M_{RH\_i} - M_{dry}}{V}, \tag{3}$$

where V indicates the volume of each sample, which was geometrically determined. Sorption isotherms were finally obtained by plotting equilibrium water contents against relative humidity during the absorption process.

3.2.4. Resistance to water vapour diffusion

The test was based on EN 1015-19 [49] and ETAG 004 [46]. It was performed in a climatic chamber, at 23 °C and 50% RH, with the cup method, for disk samples of single and painted materials, and for layered tile samples of single and combined materials (Fig. 3d). As vapour permeability depends on the conditions of humidity taken into account [70], two types of tests were performed, with the dry-cup and wet-cup settings. The dry-cup test was performed by using a desiccant (aqueous solution saturated with calcium chloride, $CaCl_2$) to create a 0% RH environment inside the cup. On the other hand, in the wet-cup test the indoor environment was kept at 100% RH by using liquid water [71]. These conditions of extreme RH were chosen to take into account

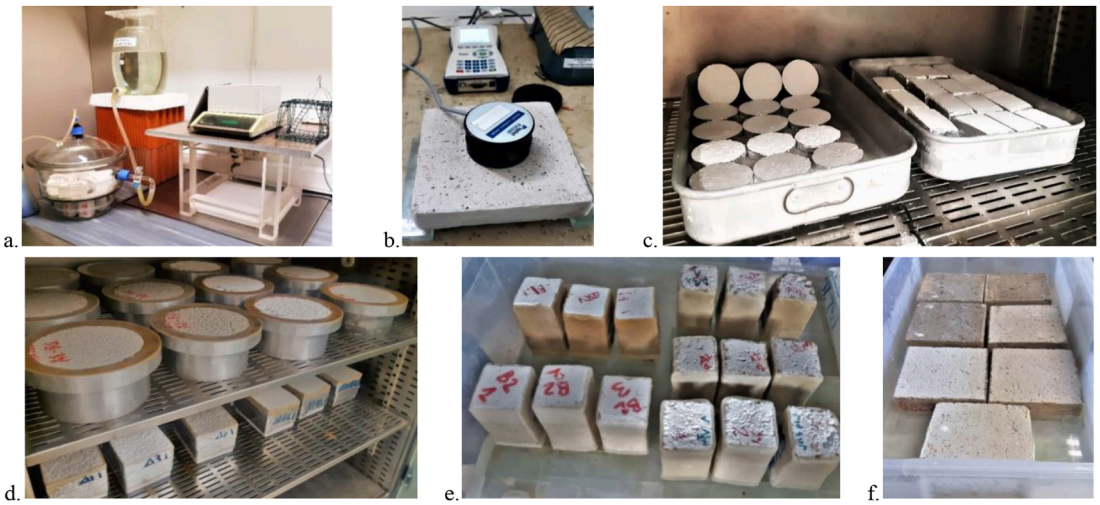

Fig. 3. Experimental campaign: apparatus for testing open porosity (a), thermal properties (b), sorption isotherm (c), water vapour permeability (d) and capillary water absorption (e, f).

the suggestions of standard EN 15803:2009 [59] for materials for application in cultural property, which recommends considering very low and/or very high RH inside the cup (namely around 0% RH and 93% RH in the standard).

To ensure that vapour flux would pass only through the horizontal surfaces of the samples, their lateral areas were sealed. Once the experimental setup was ready, periodic weighings were performed until constant vapour flux was reached in 5 successive measurements. At that point, the water vapour permeability of the sample was quantified according to Fick's law as suggested in ISO 12572:2016 [72]:

$$\delta = d \bullet \left(\frac{G}{A \bullet \Delta p_v}\right)\left[\frac{kg}{msPa}\right], \tag{4}$$

where d is the thickness of the specimen [m], G is the average vapour flux in the last 5 measurements [kg/s]; A is the exposed area of the sample [m^2] and Δp_v is the difference in vapour pressure between the horizontal faces of the sample [Pa]. Vapour pressure was derived from the temperature and relative humidity in the test:

- $Pv_0 = 0.00$ Pa, at 23 °C and 0% RH (interior surface in the dry-cup);
- $Pv_{50} = 1403.91$ Pa, at 23 °C and 50% RH (facing the controlled environment in the climatic chamber);
- $Pv_{100} = 2807.81$ Pa, at 23 °C and 100% RH (interior surface in the wet-cup).

Finally, the water vapour resistance factor was defined as the ratio between the vapour permeability of still air (δ_a) and the permeability of the sample (δ):

$$\mu = \frac{\delta_a}{\delta}, \tag{5}$$

with $\delta_a \approx 195\ 10^{-12}$ kg/(m s Pa) at 23 °C and atmospheric pressure.

For systems and paints, guidelines and standards consider the water-vapour diffusion-equivalent air layer thickness, s_d, instead of μ, which is defined as:

$$s_d = \mu \bullet d. \tag{6}$$

The s_d of paints and single layers of mortars were calculated by difference (between specimens with more and fewer layers), applying Fick's law to multi-layered samples, as shown in Ref. [73]:

$$s_{d,S} = s_{d\_air\_i} + s_{d,substrate} + s_{d\_top\_layer} + s_{d\_air\_e}, \tag{7}$$

where $s_{d,S}, s_{d\_air\_i}, s_{d,substrate}, s_{d\_top\_layer}, s_{d\_air\_e}$ are the s_d of the whole sample, of its interior surface (inside the cup), of the substrate (sample without top layer), of the top layer and of the exterior surface of the sample (the one exposed to 50% RH), respectively. The resistance of the surfaces are evaluated following the indication of Ref. [74]:

$$s_{d_{air}[m]} = \frac{1}{67 + 90v} \tag{8}$$

with v[m/s] indicating the air velocity at the surface of the sample, which is considered to be negligible inside the cup ($v_i \approx 0$ m/s, $s_{d\_air\_i} \approx 0.015$ m) and equal to the air velocity in the chamber at the exterior surface, ($v_e \approx 0.3$ m/s, $s_{d\_air\_e} \approx 0.011$ m). The air velocity in the chamber was estimated by means of a hot-film anemometer (CaTec-air velocity transmitters EE65, working range: 0–10 m/s, accuracy: ±0.2 m/s).

3.2.5. Capillary water absorption

3.2.5.1. Capillary water absorption curves. Tests on single materials were based on EN 1015-18:2002 [53] and EN 15801:2009 [57]. For each material, prism specimens (160x40x40mm) were cut into two halves and only one of them was tested. The face resulting from the cut was regularized with sandpaper and its area was geometrically determined (A). The samples were sealed along their lateral surface (to prevent evaporation during the absorption test [39,53]) and left for 24 h at controlled conditions (23 °C ± 5 °C, 50% ± 5% RH). Their initial mass was then measured (M_0) and they were positioned in a tray filled with water, on lateral supports, so that the level of water was 5–10 mm above the tested surfaces, as shown in Fig. 3e. The mass of the specimens (M_i) was periodically measured and the change of water content per unit area, (M_i-M_0)/A, was plotted versus the square root of time, $t^{1/2}$, to obtain the water absorption curves of the materials.

The testing methodology adopted for tile samples was based on ETAG 004 [46]. The procedure followed was very similar to the one adopted for prisms, except that tile samples were not cut in the process. Tile samples were sealed along their lateral surfaces, left for 24 h at controlled conditions, and then put in the trays, on lateral supports, with the tested surface 5–10 mm under the water level, as shown in Fig. 3f. The specimens were periodically weighed, and the water absorption curves were determined as for prism specimens.

3.2.5.2. Capillary water absorption coefficient. The water absorption curves can be separated into two parts. The first part describes the capillary-dominated absorption, and it can be approximated with a

Table 4
Open porosity, dry bulk density and thermal conductivity of hardened mortars (measured and declared). Specific heat capacity measured for thermal mortars.

Material	Properties declared by the manufacturers.				Experimental Results (Average ± SEM)							
	Open por. P_0 [%]	Dry bulk density ρ_{dry} [kg/m^3]		Th. Cond. λ [10^{-3} W/m K]	Open porosity P_0 [%]		Dry bulk density ρ_{dry} [kg/m3]		Th. Conductivity (10 °C, dry) $\lambda_{10°C,\ dry}$ [10^{-3} W/m K]		Sp. Heat Capacity (dry) Cp_{dry} [J/kg K]	
A1	71.64	370	± 10%	45	34.16	± 0.18	612.8	± 5.4	97.83	± 0.72	843	± 50
A2	71.64	440	± 10%	80	30.72	± 0.26	724.2	± 6.2	126.90	± 0.84	848	± 60
A3	—	350	± 50	50	28.83	± 0.46	342.3	± 6.1	65.4	± 2.8	919	± 146
B1	—	1350	± 10%	/	30.654	± 0.074	1616.5	± 1.8	/		/	
B2	—	1450	± 100	/	31.11	± 0.25	1315.5	± 7.5	/		/	

— : not declared; /: disregarded; Por.: Porosity; Th.Cond.: Thermal Conductivity.

straight line [75] whose slope is represented by the capillary water absorption coefficient (A_w) [76]. Standard EN 1015-18:2002 approximates this coefficient to be the rate between 10 min (weight M1) and 1.5 h (weight M2) of absorption. Whereas, Standard EN 15801:2009 accounts for the slope of the regression line through the first 5 measurements, and ETAG 004 considers the rate between the starting point and the water absorption at 24 h. The three coefficients were determined to allow for a comparison aimed to define what type of A_w to adopt in forthcoming numerical simulations.

4. Analysis of experimental results

4.1. Open porosity and dry bulk density

The results obtained for open porosity (P_0) and dry bulk density (ρ_{dry}) of hardened mortars are reported in Table 4, together with the values declared by the manufacturers.

All mortars have similar values of porosity, around 29–34% for thermal mortars and about 31% for regularization mortars. The values obtained with regularization mortars are in line with the P_0 experimentally observed by other authors [23,24,39], i.e. 26%-38% for plastering/rendering mortars made with cement, hydraulic lime and mixed binders. On the other hand, the open porosity observed in thermal mortars appears quite low for industrial mixes containing air-entraining admixtures, considering that other authors obtained about 70% for a lime-perlite thermal render [39] and 46–47% for commercial lime-cork mortars [24]. Similar results were instead obtained in an experimental study on cement-cork mortars where no admixtures were considered (P_0 = 38% [24]). These outcomes suggest a lack of efficacy of the air-entraining admixtures adopted in the thermal mortars analysed. This concern is further confirmed, in the case of mortars A1 and A2, by the fact that the experimentally obtained P_0 is less than half the declared value.

The dry bulk densities measured are very similar to the design values for mortars A3 and B2, and comparable for mortar B1 (with a difference of about 20%). On the contrary, the results obtained for cork-based mortars (A1, A2) are 65% higher than declared. This outcome is coherent with the reduced open porosity obtained for the two cork-mortars in comparison with the value declared in their technical sheets, which indicates a limited presence of voids in the materials and higher compactness than originally designed for. The three thermal mortars have a dry bulk density lower than 1300 kg/m^3, which is the maximum value admitted for lightweight mortars in standard EN 998-1.

The discrepancy observed in the measured and declared dry bulk density for lime-cork mortars A1 and A2 appears very relevant. For this reason, the accuracy of the measurements was investigated by repeating the test with another method and different samples. Three tile specimens of thermal mortars A1 and A2, stabilized at 23 °C ± 5 °C and 50% ± 5% RH, were considered. Their volumes were geometrically determined, and their mass measured by gravimetric weighing. The results obtained, $\rho_{dry\_A1\_tile}$ = (567.4 ± 2.2) kg/m^3 and $\rho_{dry\_A2\_tile}$ = (695.6 ± 3.9) kg/m^3, are in the same order of magnitude as those observed with prism samples, thus indicating that the dry bulk densities presented in Table 4 are in fact representative of the samples of hardened mortars A1 and A2 obtained in the laboratory.

4.2. Thermal conductivity and specific heat capacity

The thermal properties of dry thermal mortars, at 10 °C, are reported in Table 4. The measured specific heat capacity is around 850 J/(kg K) and 920 J/(kg K) for the two cork-based mortars and the one with EPS, respectively: a difference that does not seem significant, given the high variability in the C_{dry} of the EPS-mortar (high SEM). These results are in line with the value observed by Walker and Pavía [36] for a lime-cork mortar (866.50 W/kg.K) and with the ones measured by Horma et al. [77] for EPS-cement plaster composites (1000–1150 W/kg.K).

Also the results obtained for thermal conductivity are similar to the ones observed in previous studies on thermal mortars. The thermal conductivity of A3 is in line with the results obtained by Maia, Ramos, and Veiga [23] for lime and mixed-binders mortars containing EPS, which were in the range of 0.049–0.078 W/(m.K). The results of lime-cork mortars A1 and A2 are similar to those presented by Gomes et Al. [65] for lime and cement mortars containing cork aggregates, i.e. values between 0.07 and 0.10 W/(m.K). These values are also aligned with the ones observed by authors studying thermal mortars for adoption in historic buildings, such as lime-based solutions with hemp, cork and perlite, i.e. 0.07 – 0.10 W/m.K [36,39]. Furthermore, the thermal conductivities detected are more promising than those obtained in studies considering plasters based on gypsum and EPS[78] (λ = 0.12–0.22 W/(m.K)) or lime and expanded glass [37] (λ = 0.35 W/(m.K)), while they offer lower performance than solutions based on lime and advanced insulation materials such as aerogel [29] (thermal conductivity as low as 0.025 W/(m.K)).

All mortars showed higher thermal conductivities than the ones declared by manufacturers. The A3 mortar was found to be 30% higher than declared and A2 was more than 60% higher, while A1 had more than twice the declared value. For A3, the discrepancy may be related to differences in preparation and conditioning of the samples, or to a difference in the application method adopted, as observed by Govaerts et al. [39] who obtained a 50% higher thermal conductivity than declared when studying lime-perlite thermal mortars. On the contrary, for thermal mortars A1 and A2, the results are probably affected by the reduced open porosity experimentally obtained.

According to the European standard EN 998-1 [20], thermal mortars A1 and A3 can be classified as T1, i.e. thermal conductivity (λ) ≤ 0.10 W/(m.K), whereas A2 belongs to thermal class T2 ($\lambda \leq$ 0.20 W/(m.K)). Nevertheless, considering the values declared by the manufacturers, they would all be classified as T1. ETAG004 guidelines for composite thermal insulation systems set stricter requirements, defining a maximum threshold value of λ_{max} = 0.065 W/(m.K) for the insulation layer of ETICS. Thus, the thermal mortars considered only offer moderate thermal insulation capacity in comparison to typical ETICS solutions (such as EPS and mineral wool-based ones), since they exceed the λ_{max} defined by ETAG004. However, they still seem to be of interest for

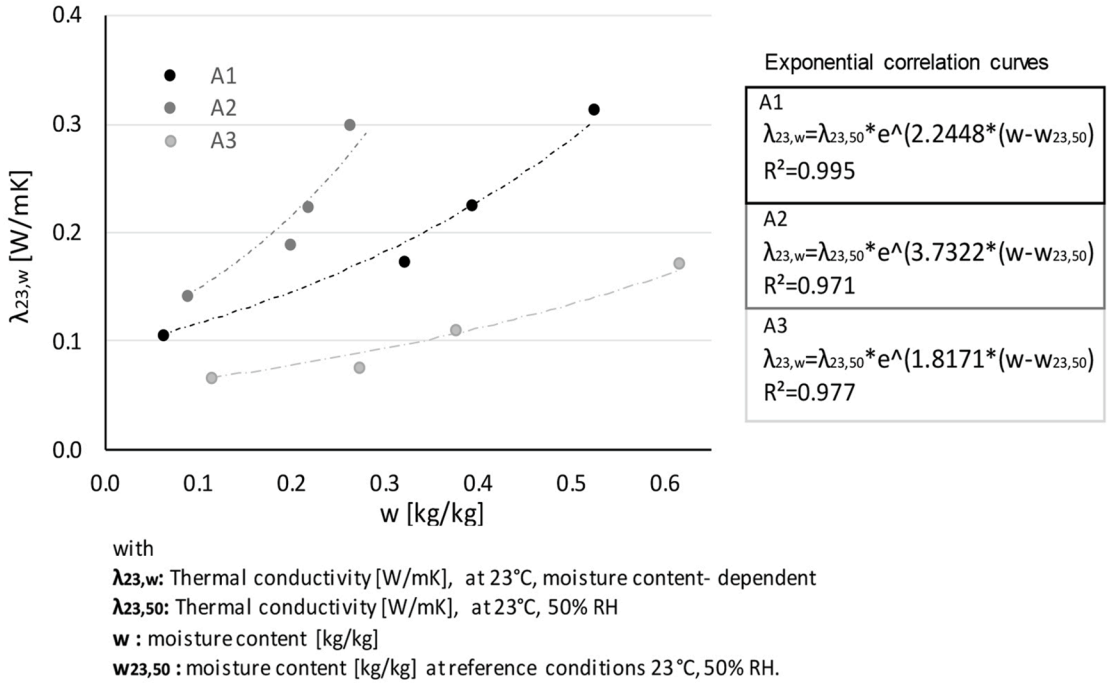

Fig. 4. Thermal conductivity of thermal mortars at different water contents and 23 °C. On the left, the graphic presents the measured data (grey and black points) and the exponential regression curves correlating thermal conductivity and water content for each thermal mortar (dashed lines). On the right, the expression and coefficient of determination of the curves are reported.

adoption in climates with moderately cold winters because they comply with the requirements set by EN 998-1 for thermal mortars, and they offer much better thermal performance than traditional renders and plasters based on gypsum, lime and cement, whose thermal conductivities are typically in the range of 0.4 – 1.0 W/(m.K) [79].

The results obtained with thermal mortars at different moisture contents are shown in Fig. 4. As expected, thermal conductivity relevantly increases when moving from lower to higher water contents. Furthermore, a strong exponential correlation ($R^2 \geq 0.97$) is found between the moisture content (mass by mass) and the thermal conductivity, normalized by its value at 23 °C, 50% RH, as suggested in standard EN ISO 10456:2007 [80].

4.3. Sorption isotherm

4.3.1. Standard samples: small disk samples of single materials and applied paints

Fig. 5a and 5b show the Sorption isotherms obtained via laboratory testing, in comparison with some results found in the literature. Cork-based mortars (A1, A2) show very similar curves while EPS-based mortar (A3) has a lower moisture absorption at all steps of relative humidity. This difference is probably due to the difference in open porosity between the first two mortars and A3, and to the hydrophobic nature of EPS. The literature indeed indicates that EPS has a lower moisture content than cork along the whole sorption curve (Fig. 5a). Regularization mortars B1 and B2 have similar moisture absorption at all steps of RH, with small but noticeable differences at 70% and 80% RH. The effect of paint C1 on regularization mortar B1 is to lower its moisture content to a very small extent, which appears to be relevant only at 95% RH. On the contrary, silicate paint C2 noticeably reduces the moisture absorbed by the sample, from 70% RH on. The results obtained for cork-based mortars are in agreement with the water content measured for a lime-cork mortar at 23 °C, 80% RH by Walker and Pavía [81]. Similarly, the moisture contents obtained for thermal mortar A3 and regularization mortars B1 and B2 are close to the values observed at 80% and 90% RH by Maia, Ramos, and Veiga [23] for a mixed binder mortar with and without EPS aggregates, respectively. Detailed results obtained with single materials and regularization mortars finished with paints are reported in Table 5 and they are the ones which are adopted for the database for numerical simulations.

4.3.2. Tile samples: Samples of complete systems

Sorption isotherms of complete systems are reported in Fig. 5c. Systems S1 (A1 + B1 + C1) and S3 (A2 + B1 + C1) present very similar behaviour, which was expected since they are regularized and finished with the same materials, and their base thermal mortars also have very similar sorption isotherms. Likewise, systems S2 (A1 + B1 + C2) and S4 (A2 + B1 + C2) present comparable moisture contents along all their sorption curves, as readable in Table 5. Furthermore, systems finished with paint C1 have higher sorption isotherms than the ones painted with C2, and S5 has the lowest equilibrium moisture content throughout the whole test.

4.4. Resistance to water vapour diffusion

4.4.1. Standard samples: Disk samples of single materials and applied paints

The vapour resistance factors obtained with standard disk samples are shown in Fig. 6 and Table 6. The results obtained with the wet-cup method are lower than with the dry-cup. This outcome is characteristic of hygroscopic materials, as they experience an increase in moisture transport at high relative humidity, because of the contribution of liquid transport effects [69,82]. With each method, thermal and regularization mortars show similar vapour resistance factors, all in the order of magnitude 10–20, which is coherent with the fact that they have comparable open porosities.

With the wet-cup settings, all thermal mortars (A1, A2, A3) comply with the restriction of EN 998-1:2017 [20] that defines a maximum vapour resistance factor of 15 for thermal mortars. For other rendering and plastering mortars, the standard only requires that materials have a μ that is equal to or lower than the one declared by the manufacturer. In this regard, mortar B1 shows, at wet testing conditions, a resistance

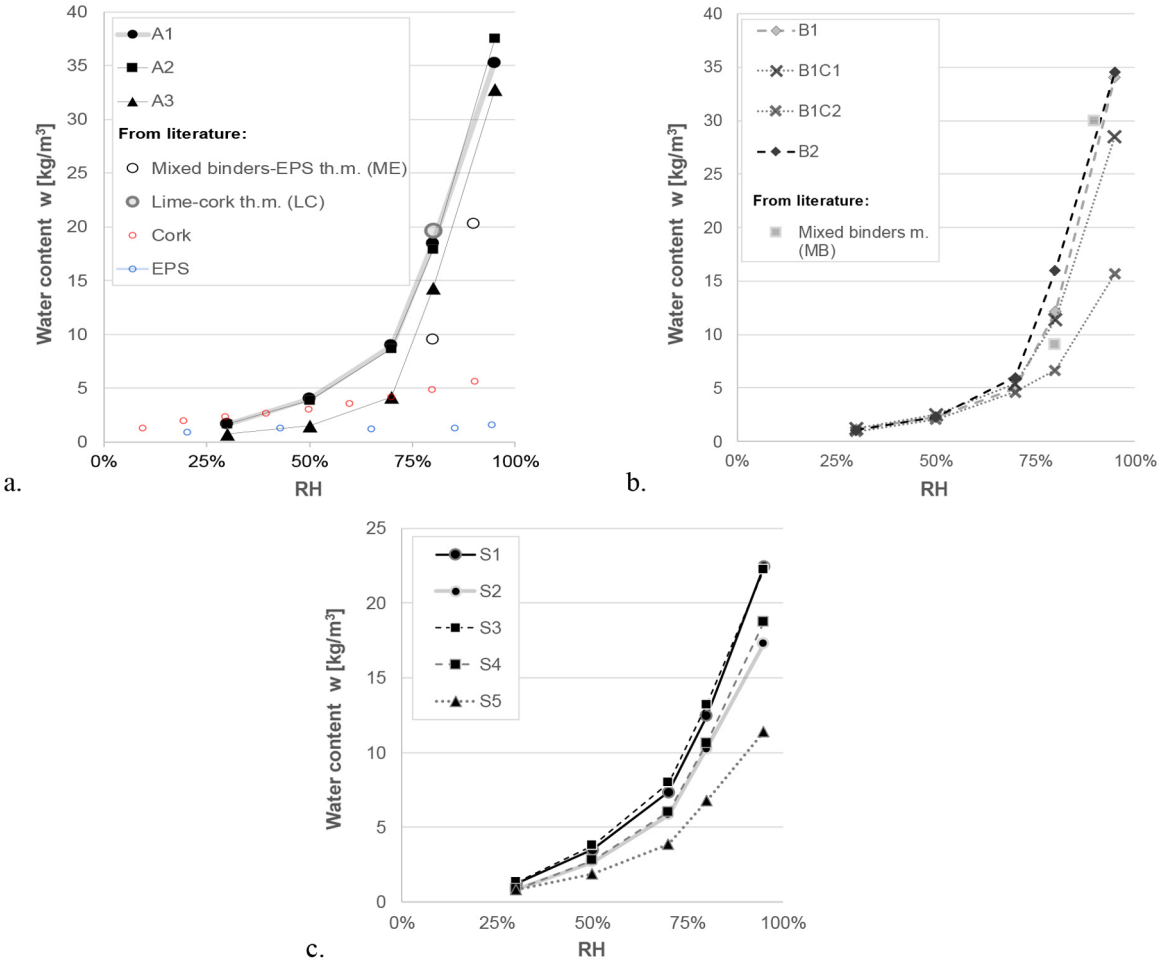

Fig. 5. Sorption isotherms of (a) thermal mortars, (b) regularization mortars with and without paints and (c) whole systems, compared to other results from the literature: cork and EPS [67], ME, MB [23] and LC [81].

Table 5
Sorption isotherms, experimental results.

	Volumetric water content, w [kg/m³]													
At RH :	*30%*			*50%*			*70%*			*80%*			*95%*		
A1	1.643	±	0.0060	3.98	±	0.041	9.0	±	0.1	18.4	±	0.25	35.3	±	0.56
A2	1.66	±	0.034	3.87	±	0.038	8.7	±	0.16	17.9	±	0.35	37.5	±	0.91
A3	0.74	±	0.031	1.53	±	0.033	4.16	±	0.075	14.3	±	0.22	33	±	1.1
B1	1.11	±	0.015	2.29	±	0.018	4.92	±	0.082	12.2	±	0.21	34.1	±	0.92
B1C1	1.20	±	0.058	2.49	±	0.079	5.4	±	0.21	11.4	±	0.46	29	±	1.4
B1C2	0.92	±	0.018	2.09	±	0.018	4.64	±	0.051	6.7	±	0.13	15.7	±	0.38
B2	1.06	±	0.037	2.29	±	0.031	5.99	±	0.034	16.0	±	0.25	34.6	±	0.75
S1	1.23	±	0.038	3.5	±	0.10	7.3	±	0.22	12.4	±	0.32	22	±	1.8
S2	0.85	±	0.045	2.7	±	0.12	5.8	±	0.22	10.2	±	0.30	17.3	±	0.48
S3	1.31	±	0.019	3.76	±	0.048	7.96	±	0.090	13.2	±	0.15	22.3	±	0.32
S4	0.87	±	0.051	2.79	±	0.091	6.0	±	0.15	10.6	±	0.12	18.8	±	0.15
S5	0.80	±	0.015	1.86	±	0.023	3.87	±	0.039	6.75	±	0.091	11.4	±	0.18

factor that agrees with the value declared by the manufacturer, i.e. $\mu \leq 15$. On the contrary, mortar B2 and all thermal mortars have resistance factors which are more than double the declared value ($\mu_{declared} \leq$ 4–5), at wet conditions.

Even though paints C1 and C2 are both declared to be "breathable", they give very different results when applied on samples of regularization mortar. C1 has a negligible effect (a maximum of 5% increase in μ of the finished sample) while C2 causes a strong increase of the resistance factor of the samples, especially at dry conditions (5 times higher μ than in the unfinished specimens). Hence, silicate-paint C2 shows much higher resistance to vapour diffusion than lime-paint C1.

The results obtained for regularization mortars are aligned with a previous study on cement-based mortars, where industrial and traditionally prepared mixes gave μ-values of about 8.2–14 and 18, at wet testing conditions [83]. Furthermore, the results obtained have the same order of magnitude of the resistance factors observed by Veiga et al. [50] with mortars based on cement and air lime, i.e. μ-values in the range of 4.6–6.0. The vapour resistance factors obtained with the specimens of thermal mortars are similar to those observed in previous studies, i.e. 7.5–13.5 for cork and EPS thermal renders [23] and around 10–20 for

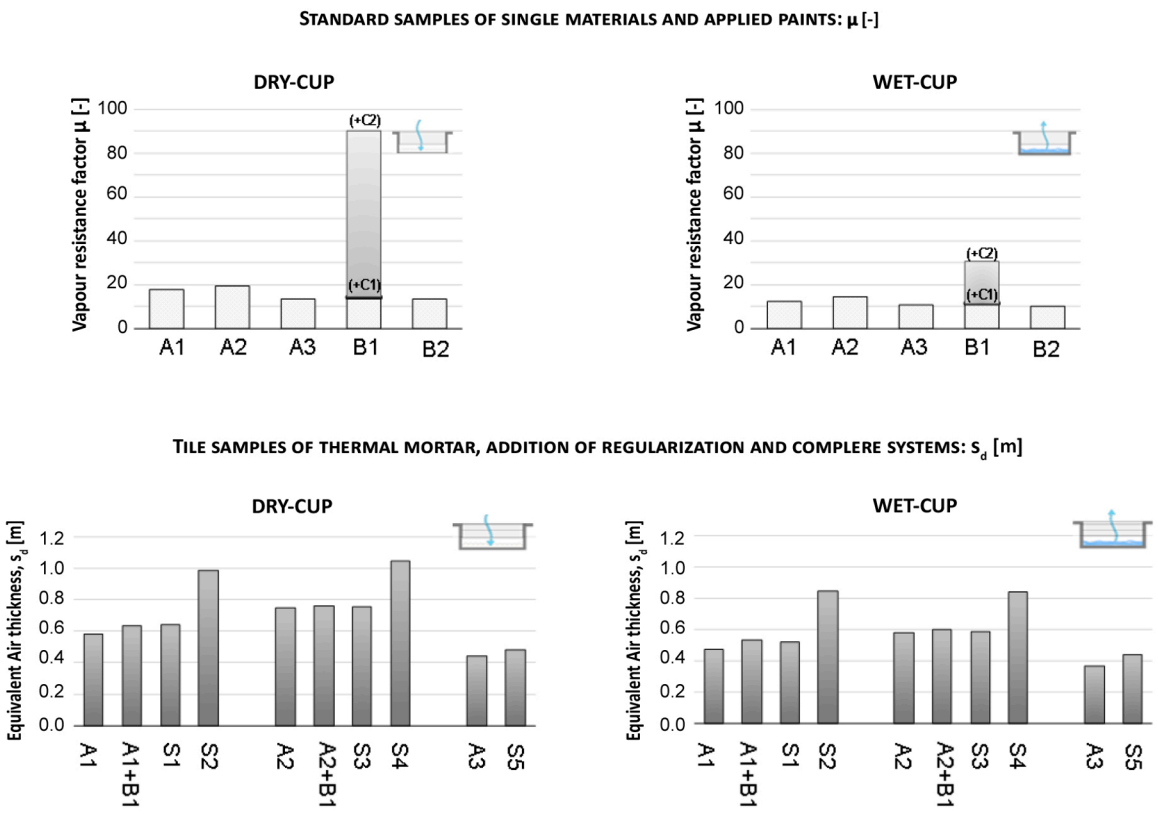

Fig. 6. Resistance to water vapour diffusion, experimental results.

Table 6
Resistance to water vapour diffusion, experimental results.

Standard samples of single materials and applied paints												
Direct measures							*Indirect measures (difference with substrate)*					
Vapour resistance factor, μ [-]							*Equivalent air thickness of paints, Sd [m]*					
	Dry - cup			*Wet - cup*				*Dry - cup*			*Wet - cup*	
A1	**17.8**	±	0.97	**12.1**	±	0.19						
A2	**19.1**	±	0.68	**14.3**	±	0.06						
A3	**13.3**	±	0.82	**10.7**	±	0.98						
B1	**13.6**	±	0.36	**11.1**	±	0.07						
B1 + C1	**14.3**	±	0.46	**11.2**	±	0.91	→ **Sd_C1**	**0.020**	±	0.0090	**0.01**	± 0.010
B1 + C2	**90**	±	14	**30.4**	±	2.2	→ **Sd_C2**	**1.5**	±	0.26	**0.38**	± 0.041
B2	**13.2**	±	0.18	**10.1**	±	0.18						
Tile samples - thermal mortar, addition of regularization and complete systems.												
Direct measures							*Direct* and Indirect measures (difference with substrate)*					
Equivalent air thickness, Sd [m]							*Vapour resistance factor of mortars, μ [-]* *Equivalent air thickness of paints, Sd [m]*					
	Dry - cup			*Wet - cup*				*Dry - cup*			*Wet - cup*	
A1	**0.58**	±	0.014	**0.47**	±	0.016	→ **μ_A1***	**14.6**	±	0.29	**12.0**	± 0.49
A1 + B1	**0.633**	±	0.0092	**0.533**	±	0.0044	→ **μ_B1**	**20**	±	2.4	**12**	± 1.8
S1	**0.642**	±	0.0013	**0.519**	±	0.0008	→ **Sd_C1**	**0.058**	±	0.0042	**0.035**	± 0.0016
S2	**0.98**	±	0.037	**0.84**	±	0.019	→ **Sd_C2**	**0.41**	±	0.039	**0.37**	± 0.022
A2	**0.747**	±	0.0090	**0.584**	±	0.0080	→ **μ_A2***	**18.8**	±	0.26	**14.7**	± 0.22
A2 + B1	**0.759**	±	0.0080	**0.60**	±	0.013	→ **μ_B1**	**16**	±	1.8	**15**	± 2.7
S3	**0.75**	±	0.017	**0.59**	±	0.026	→ **Sd_C1**	**0.048**	±	0.0071	**0.04**	± 0.019
S4	**1.04**	±	0.058	**0.84**	±	0.018	→ **Sd_C2**	**0.33**	±	0.062	**0.28**	± 0.024
A3	**0.44**	±	0.020	**0.37**	±	0.016	→ **μ_A3***	**11.0**	±	0.52	**9.2**	± 0.44
S5	**0.48**	±	0.010	**0.40**	±	0.014	→ **μ_B2**	**16**	±	3.0	**14**	± 3.5

*For A1, A2, and A3, the vapour resistance factor is directly measured from the results obtained with tile samples made of thermal mortars. For regularization mortars (B1, B2) and paints (C1, C2) the results are obtained indirectly.

hemp-lime plasters [27], at dry testing conditions.

On the other hand, the experimentally observed results are worse (higher resistance to vapour diffusion) than the ones obtained in a study [35] on thermal mortars made of various binders, glass fibre reinforced polymer powder (GFRP) and air-entraining additives, i.e. μ-values in the range of 1.2–6.6. In this case, the authors inferred that the combined use of additives and GFRP powder improved the level of entrapped air in the mortars, which is probably why they obtained much better results than the ones hereby observed with thermal mortars which have a moderate open porosity.

The s_d measured for paints is in agreement with the results obtained in other studies where various silicate-paints were tested at wet conditions (s_d around 0.4–0.6 m) [84] and lime-paints were analysed with the dry-cup method (s_d of about 0.01–0.03 m) [85].

4.4.2. Tile samples: Samples of thermal mortar, addition of regularization, and complete systems

The water-vapour diffusion-equivalent air layer thickness (s_d) measured with tile samples is reported in Fig. 6. The results obtained with both the dry and wet-cup show that the addition of regularization mortars (B1, B2) and lime-paint C1 leads to very small increases of s_d, with a maximum difference of about 10% between the samples of thermal mortars and the ones completed with B1 and C1. By contrast, the use of silicate-paint C2 causes a high increase of s_d: systems S2 and S4 have about 40% to 50% higher s_d-values than unfinished samples. Nonetheless, all systems do comply with the threshold value indicated by ETAG 004 [46], i.e. $s_d \leq 1.0$ m at wet conditions (wet-cup with 93% RH in the guidelines).

It is worth highlighting that ETAG004 does not set a requirement on the vapour permeability of complete systems, but it does for the s_d of the rendering systems applied on ETICS. Thus, this is the threshold value hereby adopted as a reference. Furthermore, the maximum s_d recommended by ETAG004 depends on the type of insulation material adopted in the system, namely cellular plastic or mineral wool. In this study, the value considered is the one set for mineral wool-based insulation as it is a vapour-permeable material, similarly to the thermal mortars hereby considered.

The detailed results obtained for tile samples, as well as the resistance of the paints indirectly measured, are reported in Table 6. The s_d obtained for paints confirms that C2 is much less permeable than C1: according to EN 1062–1:2004 [86], the vapour permeability of the two paints can be respectively classified as medium (V_2: $0.14 \leq s_d < 1.4$) and high (V_1: $s_d \leq 0.14$). The magnitude of the results is consistent with the outcomes of previous studies: s_d values in the range of 0.4–0.6 m were measured for various silicate-paints in Ref. [84] and increases of 0.01–0.03 m in the s_d of samples were detected when two types of lime-paints were applied to them, in Ref. [85].

Similar but not completely compatible results are observed with paints applied in different systems. On one hand, the results obtained for the s_d of paint C1 from samples of system S1 and S3 are compatible. On the other hand, the results obtained for C2 from samples of S2 and S4 are compatible only at dry conditions. This fact can be related to the higher uncertainties that are involved in the wet-cup method, which is considered less reliable than the dry-cup because of the sensitivity of the results to changes in relative humidity and surface resistance at the inside-exposed surface of the samples [82].

The results obtained for the systems are similar to those observed in a previous study on insulation solutions based on thermal mortars with EPS and cork aggregates [23]. In this study, the authors obtained s_d of about 0.4–1.2 m and 0.4–1.0 m, at dry and wet test conditions, respectively (results approximatively converted from the original values referring to 20 mm-thick samples, by adopting a conversion factor of 2). Comparable results were also obtained in a study on an aerogel render-based solution [87], where the equivalent air thickness of the whole system, finished with impermeable epoxy paint, was about 1.0 m at dry conditions (value roughly converted from the original result referring to 25 mm-thick samples). Finally, it is worth highlighting the scarcity of literature considering the vapour permeability test on complete insulation systems based on thermal mortars, which is probably a consequence of the standard requirements of EN 998-1, which does not account for the behaviour of complete systems, but only single mortars.

4.4.3. Standard and tile samples: Comparison of results and values selected for the database for numerical simulations

The vapour resistance factors of mortars, obtained from tile and standard samples, are provided in Table 6. Results show that the resistance factors have some variability according to the type of samples adopted. In particular, the results obtained with tile specimens of thermal mortars were very similar to the ones resulting from testing disk samples (2%-18% differences at dry conditions). Thus, the difference in geometry and construction of samples via double layering does not appear to have affected the results to a relevant extent. For regularization mortars, the differences are more important, with tile samples giving 20–30% higher s_d than standard ones. In this case, the application of the mortars on a porous support and the definition of the results by indirect measurement had a more evident influence on the test outcomes; however, results are still comparable. A much more important difference is found between the results obtained for paints applied on disk and tile supports, especially for paint C2, whose s_d is about 4-times higher with disk samples than with tile ones.

In summary, the different samples adopted (standard disks and layered tiles) gave quite comparable results for the resistance to water vapour of mortars and very different results for paints, especially C2. This outcome appears coherent with the observations presented in previous studies which stated that:

- the permeability to water vapour of paints can noticeably depend on the substrate adopted [70];
- the use of layered samples of mortars can affect the porosity of the specimen, because of the suction that the first hardened layer (porous support) may exert on the water contained in the fresh mortar applied on it [88].

Thus, samples obtained from moulds (standard samples) and from the application of successive layers of mortars (composite tile samples) can show differences in their physical properties, potentially leading to different vapour permeability of the paint-layer applied to them. The geometry of the samples may have also played a role in leading to different results with different types of samples. However, given that specimens of the same material (thermal mortars) gave quite comparable results, regardless of the shape of the samples (disks and tiles), the influence of the geometry is considered of minor importance.

Even though the results obtained with standard disk samples offer higher accuracy, thanks to the direct measurements performed, the values obtained indirectly for single materials, from tile samples, are selected for the database for numerical simulations. Indeed, layered tile samples, and the results obtained with their use, are considered to be more representative of real applications. For B1, C1 and C2, the resistance to water vapour selected for the database for numerical simulations is the average of the results obtained from the application on different supports (supports A1 and A2 for application of B1, supports A1 + B1 and A2 + B1 for paints C1 and C2).

4.5. Capillary water absorption

4.5.1. Standard samples: Prism samples of single materials

The capillary water absorption curves obtained for single materials are presented in Fig. 7a and 7b. Lime-cork mortars A1 and A2 have absorption rates that are in line with their open porosities, meaning that the higher the open porosity, the faster the water absorption. Concerning thermal mortar A3, it shows a different behaviour, having a higher water content than mortar A2 in the first hours of the test. This result

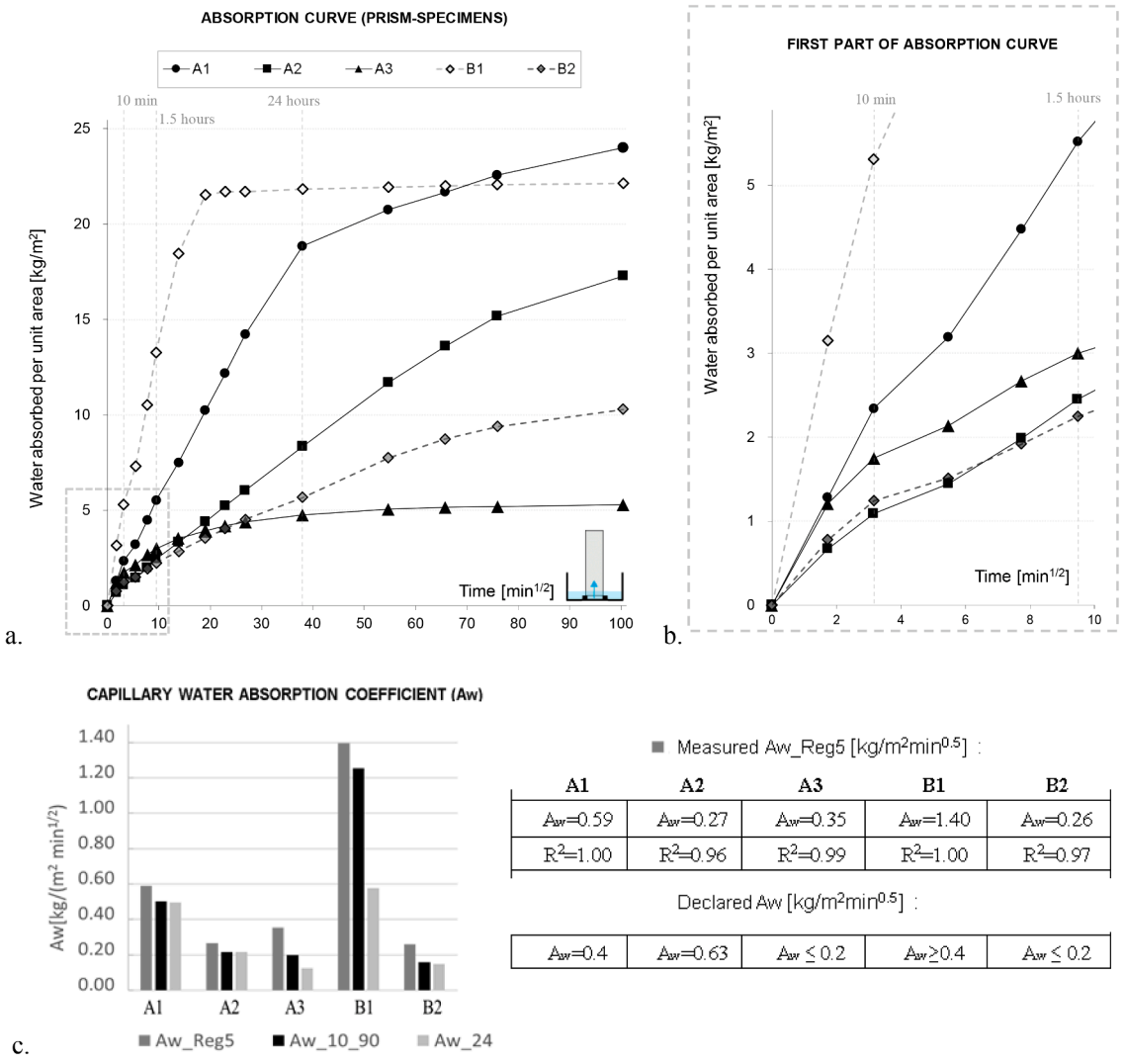

Measured Aw_Reg5 [kg/m²min^0.5] :

A1	A2	A3	B1	B2
A_w=0.59	A_w=0.27	A_w=0.35	A_w=1.40	A_w=0.26
R^2=1.00	R^2=0.96	R^2=0.99	R^2=1.00	R^2=0.97

Declared Aw [kg/m²min^0.5] :

A_w=0.4	A_w=0.63	$A_w \leq 0.2$	$A_w \geq 0.4$	$A_w \leq 0.2$

Fig. 7. Capillary absorption curves of single materials (prism specimens).

suggests that even though A3 has a lower total volume of interconnected pores than A2, it has a higher share of them in the large capillary range [89]. After 3 h of absorption, A3 has a lower moisture content than A2. This behaviour is clearly readable in the capillary water absorption coefficients reported in Fig. 7c, where A3 has a higher absorption rate than A2 in the first 5 measurements and a lower one at 24 h. From 24 h on, A3 shows the lowest water content among the tested materials, which is probably the result of both the reduced porosity of the material and the hydrophobic nature of EPS aggregates. In addition, this outcome is aligned with the results obtained by Gomes et Al. [24], who observed a significantly higher reduction of water absorption in mortars containing EPS than in those containing cork aggregates.

Regularization mortars B1 and B2 have similar open porosities, i.e. around 31%, but they have very different absorption rates: at 24 h, the water content of mortar B1 is almost four times higher than in mortar B2. The reduced water absorption of the latter material can be explained by the presence of hydrophobic agents, which is very likely since B2 is designed for direct exposure to outdoor climate.

The capillary water absorption coefficients determined with the three different methods specified in EN 15801, EN 1015–18 and ETAG 004 are presented in Fig. 7c. In all cases, the value obtained with the first 5 measurements (A_{w_Reg5}) is the highest, and the value that accounts for the average absorption rate at 24 h is the smallest (A_{w24}). This result clearly shows that the absorption curves have slopes that flatten with time, meaning that the absorption rate decreases while passing from dry to saturated conditions. Furthermore, it emerges that the coefficient obtained at 24 h is not representative of the materials analysed, as some of them (A3 and B1) reach saturation before this time.

The coefficients A_{w_Reg5} and the coefficient of determination of the regression lines are also reported in Fig. 7c. According to these results, mortars A2, A3 and B2 have an absorption coefficient lower than 0.40 kg/(m^2.min$^{1/2}$), and thus they belong to the absorption class W1, while A1 and B1 belong to the class W0 of standard EN 998-1 [20]. Mortar A1 does not comply with standard requirements as the coefficients determined with the three methods are all above the reference threshold value recommended for thermal mortars (0.40 kg.m^{-2}.min$^{-1/2}$). This result is likely to be related to the low open porosity experimentally obtained, which suggested a lack of efficacy of the air-entraining admixtures, with consequent reductions of the macropores in the mortar, as well as of their effect on lowering the capillary water absorption coefficient of the material [35].

Standard 998-1 does not indicate restrictions on the water absorption of mortars for general renders and plasters, like B1 and B2, allowing all types of absorption coefficients for them. Regularization mortar B1 has the highest capillary absorption coefficient among the analysed materials, as expected. It is in fact declared to be above 0.4 kg/(m^2 min$^{1/2}$) in its technical sheets.

Mortars A3 and B2 have a declared capillary absorption coefficient of

less than 0.2 kg/(m^2 min$^{1/2}$), which is not far from the A_{w_Reg5} obtained and, additionally, it is in strong agreement with the $A_{w\_10\_90}$ determined, which is the type of coefficient declared in technical sheets, according to standard EN998-1 and EN1015-18.

The absorption coefficient obtained for A1 is higher than the manufacturer's declared value, while the coefficient obtained for mortar A2 is lower. These discrepancies are imputable to a different method of preparation of the samples between this study and the one carried out by the manufacturers (e.g. spatula or spray application of mortars) with consequent differences in physical properties, as already observed when analysing the results of open porosity.

The results obtained for the mortars analysed are similar to the ones observed by Maia, Ramos and Veiga [23]. The authors reported coefficients of 0.1–0.23 kg/(m^2 min$^{1/2}$) for thermal renders with cork and EPS aggregates and 0.05–1.6 kg/(m^2 min$^{1/2}$) for regularization mortars. Other authors observed great variability in the results obtained with industrial thermal mortars with cork and EPS [24], namely 0.2–1.0 kg/(m^2 min$^{1/2}$). Also in this case, the values obtained in aforementioned study are in the same order of magnitude as the values hereby presented for mortars A1, A2 and A3.

4.5.2. Tile samples: Samples of thermal mortars, addition of regularization, and complete systems

Water absorption curves obtained for tile specimens of whole systems are presented in Fig. 8a and 8b. Results show that systems S2 and S4 have much smaller water content than S1 and S3, throughout the whole test. This difference is clearly related to the different use of paints: C2 in S2 and S4, C1 in S1 and S3. This outcome confirms the water-repellent nature of C2, which is indeed designed to finish outdoor-exposed components. Regarding S5, the system is designed for both indoor and outdoor exposure. It shows a high water content in the first 45 min of the test, which is similar to the moisture content in systems S1 and S3. From that point on, S5 has a lower water content than S1 and S2, and it reaches saturation before 24 h, with the lowest saturation water content per unit area of all the systems. Hence, S5 shows a very reduced moisture content in the long run, but not in the first hour of wetting. For this reason, it is a system that may experience high water absorption when subjected to short periods of rain.

In Fig. 8c, the coefficients obtained at 24 h for whole systems are presented (A_{w_24}). All systems designed for outdoor exposure, i.e. S2, S4 and S5, exceed the limitations recommended by ETAG 004, which is an A_{w_24} lower than 0.013 kg/(m^2 min$^{1/2}$), explicitly indicated in the guidelines as a maximum water content of 0.5 kg/m^2 at 24 h. The coefficients obtained at 24 h for the systems indicate that C1 can be ranked as highly water permeable ($A_{w\_24} > 0.065$ kg.m^{-2}.min$^{-1/2}$) and C2 as mediumly permeable (0.065 kg.m^{-2}.min$^{-1/2}$ $\geq A_{w\_24} >$ 0.013 kg.m^{-2}.min$^{-1/2}$), according to standards EN 1062-1:2004 [86] and EN 1062-3: 2008 [52] for paints and varnishes.

The capillary absorption contents obtained with the regression line through the first 5 measurements (A_{w_Reg5}) with all tile samples (thermal mortars, thermal mortar and regularization, and whole systems) are reported in Fig. 8c as well, and they are discussed in comparison with the results obtained for standard prism samples in the following section. It is worth highlighting that the A_{w_Reg5} reported in Fig. 8c for mortar A3 was calculated considering only the first three points of the absorption curve, due to the fact that tile samples of A3 appeared to get close to saturation after the third measurement.

Results obtained with complete systems designed for outdoor exposure (S3, S4 and S5) appear to perform worse than the solutions considered in previous studies on thermal rendering systems, where much lower capillary absorption coefficients were measured. Indeed, Maia, Ramos and Veiga [23] observed water absorption coefficients as low as 0.012 kg/(m^2 min$^{1/2}$) with solutions based on industrial thermal renders with cork and EPS, while a coefficient of 0.010 kg/(m^2 min$^{1/2}$) was observed by Pedroso et Al. [87] with an aerogel render-based solution finished with impermeable epoxy paint.

Finally, it is worth highlighting the scarcity of literature considering the capillary water absorption test on complete insulation systems based on thermal mortars. Also in this case, the lack of literature is considered to be a consequence of the standard requirements of EN 998-1, which does not account for the behaviour of complete systems, but only single mortars.

4.5.3. Standard and tile samples: Comparison of results and values selected for the database for numerical simulations

The coefficients obtained for thermal mortars with tile samples

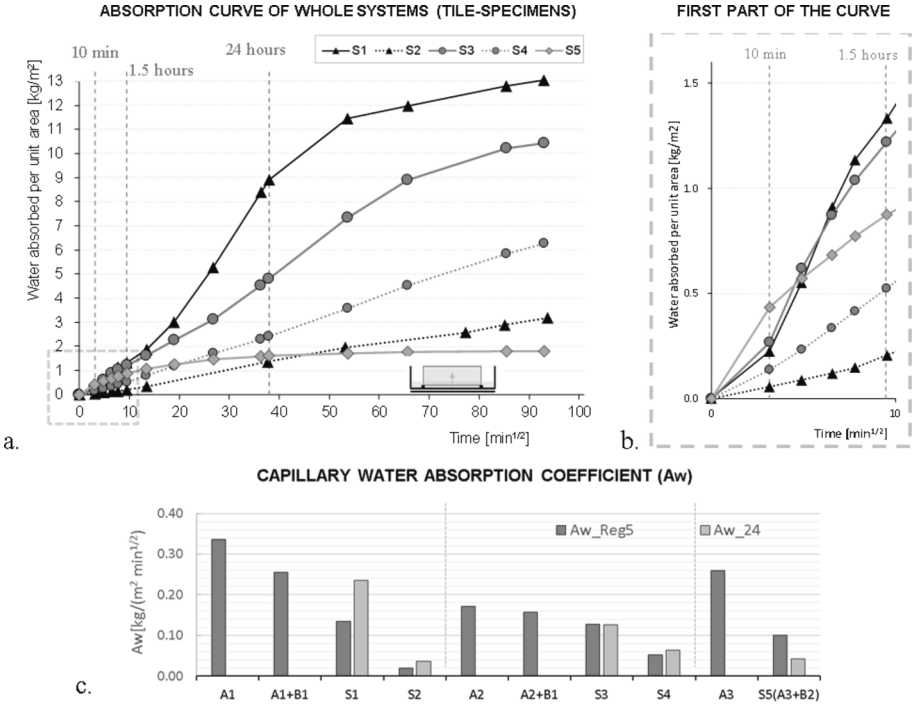

Fig. 8. Capillary water absorption, results obtained with tile samples.

(A_{w_Reg5}) are noticeably smaller than the ones obtained with prism specimens (35–75% reductions). This result reflects the differences in the geometry of the samples and their construction, as the tile-shaped ones are prepared with two successive layers of thermal mortar, a construction that tends to reduce water absorption according to a study of Silveira et Al. on cement mortars [90]. With this type of preparation, each layer (from the second one on) is applied on a previously hardened one, which acts as a porous substrate. As explained by different authors [88,90], the suction exerted by a porous substrate on the water contained in the layer of fresh mortar causes a pore tightening in this material, which has an effect on its water absorption capabilities. The authors also indicate that the higher the porosity of the substrate, the stronger it affects the applied mortar, which is consistent with the result hereby presented. Indeed, A1 has the highest open porosity and the strongest decrease of absorption coefficient from prism to tile samples, i.e. about 75%, followed by A2 and A3 with reductions of around 55% and 35%. Furthermore, the construction by successive layers gives rise to the presence of interfacial hygric resistances in-between, which can further reduce liquid water transport [91,92].

A similar reduction of capillary absorption is likely to affect also the performance of regularization mortars. Indeed, although a high absorption coefficient is observed with prism samples of B1, the application of this mortar on samples of thermal mortars A1 and A2 does not imply an increase in the water absorption coefficient of the samples, but quite the opposite. This result suggests a reduction in the absorption capabilities of B1, due to the application on a porous support, together with the presence of interfacial hygric resistances between successive layers in the assembly.

The capillary water absorption coefficients considered for the database for numerical simulations are those obtained from the regression line through the first five measurements. This choice is taken to avoid underestimating the absorption of liquid water during short periods of rain. This aspect is indeed very relevant as moisture is the most important in-service degradation agent [83], and it can lead to serious damage in the walls [93]. For thermal mortars, the results obtained with tile samples are the ones selected, as they appear more representative of real applications. For regularization mortars, the A_w can not be extrapolated from the results obtained with tile-layered samples, thus the value adopted is the A_{w_Reg5} of standard specimens. For paints, the results obtained with the application of the two finishings on tile samples (complete systems) are adopted. In particular: for C1 the value is obtained from the average A_{w_Reg5} of systems S1 and S3, and C2 is taken as the average of systems S2 and S4.

5. Synthesis and discussion of experimental results

5.1. Performance of materials and systems in comparison with standard requirements

The results experimentally obtained are summarized in Table 7, in comparison with the standard threshold values set in the standards EN 998-1 and ETAG 004. In the table, "V" and "X" are adopted to indicate if the requirements were fulfilled or not, respectively.

5.2. Synthesis of results: database for numerical simulations

The extensive experimental campaign presented in this study allowed the definition of a complete hygrothermal characterization of materials and systems to be used in numerical simulations. The data obtained is synthesized in Table 8. The database provided can be of great help to future studies focused on the efficacy and compatibility of thermal mortar-based systems for application on historic walls, as shown in a preliminary study presented by the authors [95].

5.3. Discussion of results

5.3.1. Results obtained with different types of samples

Different types of specimens were adopted for the experimental campaign: standard samples of single and painted materials and tile samples, prepared by layers, which better represent real applications and complete systems. The first typology is based on the European specifications for mortars for masonry EN 998-1 and the second one is aligned with the requirements of the European guidelines for external thermal insulation composite systems ETAG004. The results obtained led to the following observations:

- the use of layered-tile and standard samples did not result in relevant differences in terms of **vapour permeability** of mortars, but it did for paints, especially for C2 at dry conditions. In the latter case, the s_d obtained with standard samples was 4-times higher than the one obtained with tiles. This outcome is coherent with a previous study [70] which observed that the resistance of paints to vapour diffusion can noticeably depend on the substrate adopted;
- relevant **reductions of capillary water absorption** were obtained with tile layered samples of thermal mortars, with A_w coefficients 75%-35% lower than in standard samples. Similar differences have been observed also in previous studies [88,90] which indicate that sample preparation can affect the physical properties of mortars, especially when they are applied on porous supports (for example the previously hardened layer) that can absorb water from the fresh mortar applied. Furthermore, in samples prepared by successive layers, the effect of hygric resistances at the interfaces [92] between

Table 7
Compliance of mortars and insulation systems with standard requirements (EN 998-1, ETAG004).

Standard requirements	materials					systems				
	A1	A2	A3	B1	B2	S1	S2	S3	S4	S5
- Resistance to water vapour diffusion										
EN 998-1: μ-value (wet-cup) ≤ 15 for TM	V	V	V	–	–	–	–	–	–	–
ETAG004: s_d (wet-cup) ≤ 1.0 m	–	–	–	–	–	V	V	V	V	V
- Capillary water absorption										
EN 998-1: Aw ≤ 0.40 kg.m^{-2}.min$^{-1/2}$ for TM	X	V	V	–	–	–	–	–	–	–
ETAG004: Aw_{24} ≤ 0.013 kg.m^{-2}.min$^{-1/2}$	–	–	–	–	–	–*	X	–*	X	X
- Thermal conductivity										
EN 998-1: λ ≤ 0.20 W/(m K) for TM	V	V	V	–	–	–	–	–	–	–
ETAG004: λ ≤ 0.065 W/(m K)	–	–	–	–	–	X	X	X	X	X

TM: thermal mortars, V: verified, X: failed, -: not applicable, -*: not considered for internal insulation systems.

Table 8
Characteristic of thermal insulation systems and properties of the materials for numerical simulations.

Thermal insulation systems:			
Systems		**Side of insulation**	**Composition of the system**
S1	based on cork-mortar A1	INTERIOR	th.m. A1 (4 cm) + reg.m. B1 (2 mm) + paint C1 (0.5 mm)
S2	based on cork-mortar A1	EXTERIOR	th.m. A1 (4 cm) + reg.m. B1 (2 mm) + paint C2 (0.5 mm)
S3	based on cork-mortar A2	INTERIOR	th.m. A2 (4 cm) + reg.m. B1 (2 mm) + paint C1 (0.5 mm)
S4	based on cork-mortar A2	EXTERIOR	th.m. A2 (4 cm) + reg.m. B1 (2 mm) + paint C2 (0.5 mm)
S5	based on EPS-mortar A3	INTERIOR/EXTERIOR	th.m. A3 (4 cm) + reg.-finishing m. B2 (2 mm)

th. = thermal, m. = mortar, reg. = regularization

Materials adopted in the insulation systems:							
	A1	**A2**	**A3**	**B1**	**B2**	**C1**	**C2**
DRY BULK DENSITY [kg/m^3]	612.8	724.2	342.3	1617	1316	1617	1617
OPEN POROSITY [m^3/m^3]	0.342	0.307	0.288	0.307	0.311	0.307	0.307
VAPOUR RESISTANCE FACTOR [-]						*For layers of paint 0.5 mm thick:*	
dry conditions	14.6	18.8	11.0	18.3	15.6	106	737
wet conditions	12.0	14.7	9.17	13.4	13.7	72.5	648
CAPILLARY WATER ABSORPTION COEFFICIENT [kg/(m^2 s$^{0.5}$)]	0.044	0.022	0.034	0.181	0.034	0.017	0.005
FREE WATER SATURATION Wsat [kg/m^3]	300.0	215.9	66.2	276.7	128.6	276.7	276.7
MOISTURE STORAGE FUNCTION/SORPTION ISOTHERM (w [kg/m^3])							
at RH 30%	1.64	1.66	0.74	1.11	1.06	1.20	0.92
at RH 50%	3.98	3.87	1.53	2.29	2.29	2.49	2.09
at RH 70%	8.97	8.71	4.16	4.92	5.99	5.40	4.64
at RH 80%	18.42	17.91	14.30	12.18	16.02	11.42	6.69
at RH 95%	35.27	37.52	32.84	34.07	34.58	28.57	15.71
at RH 100%	300.0	215.9	66.2	276.7	128.6	276.7	276.7
REFERENCE WATER CONTENT w_{80} [kg/m^3]	18.42	17.91	14.30	12.18	16.02	11.42	6.69
SPECIFIC HEAT CAPACITY [J/kg K]	843	848	920	*850	*850	*850	*850
THERMAL CONDUCTIVITY Dry [W/mK]	0.098	0.128	0.065	*0.7	*0.7	*0.7	*0.7

THERMAL CONDUCTIVITY						
moisture dependent λ(w)	**A1**		**A2**		**A3**	
	w	**λ**	**w**	**λ**	**w**	**λ**
at w0 (50% RH)	33.0	0.107	59.7	0.142	31.7	0.067
at w1	171	0.175	133	0.190	75.9	0.076
at w2	210	0.226	148	0.224	105	0.111
at w3	280	0.315	181	0.300	171	0.171
****at saturation**	342	0.325	307	0.498	288	0.249
	with λ [W/mK] and w [kg/m3]					

*assumed from typical values found in lime-mortars from Wufi database [94]. **extrapolated from the exponential correlations λ-w.

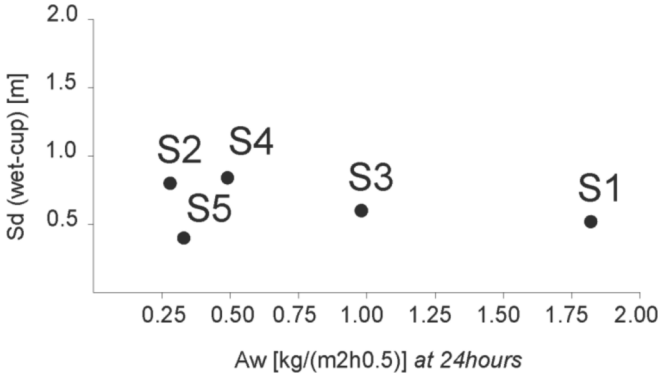

Fig. 9. A_w (at 24 h) and s_d (wet cup) obtained for the complete systems.

layers may have further contributed to reducing the capillary water absorption coefficient of the specimens.

These outcomes show that complete insulation systems may have very different moisture transport properties than expected from the characterization of single materials. Thus, it would be beneficial to add some information concerning the behaviour of complete systems, as whole units, in the technical sheets of thermal mortar-based insulation solutions: namely the s_d for all systems, and also the A_w for those designed for outdoor exposure. This additional information would allow designers to make a much more informed choice and to better forecast the realistic impact of the system on the moisture dynamics of the wall, potentially leading to reduced degradation risks and improved durability of the retrofitted components.

5.3.2. Properties of complete systems

In terms of the properties of complete insulation systems, the following information was obtained:

- systems intended for external application showed a lower capillary water absorption than those designed for interior exposure (S3, S1), due to the reduction of water intake provided by the finishing layer: paint C2 (in system S2, S4) or mortar B2 (in system S5). Nonetheless, the three systems (S2, S4, S5) did not comply with the maximum capillary water absorption defined by the European Guideline for external thermal insulation composite systems with rendering - ETAG 004;
- regularization and finishing may strongly impact the hygric performance of the systems, resulting in characteristics that are very different from those of the insulation layer. For instance, systems that differ only in the finishing layer (S1-S2 and S3-S4) resulted in having 40%-60% higher Sd (at wet conditions) when paint C2 was used instead of C1, even though they were both declared to be "breathable" finishings. This outcome is clearly observable in Fig. 9, where the capillary absorption coefficient and resistance to vapour diffusion of the complete systems are synthesized;
- the sorption isotherms obtained with samples of complete systems showed that the use of different finishings can noticeably affect the sorption isotherm of the solutions: the use of paint C1 (in systems S1 and S3, designed for internal interventions) resulted in the highest moisture content along the whole range of RH considered (30%-95%). This feature appears positive for systems adopted on the interior side of walls as it can help to improve indoor hygrothermal comfort [14].

5.3.3. Thermal performance and dependency on water content

The thermal mortars analysed complied with the restrictions set by EN 998-1 for the thermal conductivity of thermal mortars, while they exceeded the maximum value allowed by ETAG 004 for ETICS. Thus, while they have lower thermal insulation capacity than typical ETICS, they still offer much better performance than traditional plasters and renders based on gypsum, lime and cement, and so they appear to be promising for application in climates with moderately cold winters.

Experimental results showed that the influence of water content on thermal conductivity was very significant. This aspect appears to be relevant, and it should be indicated and quantified in the technical sheets of thermal mortars, especially if they are designed for external insulation systems, as they may experience relatively high water content during some periods of the year, which could lead to poor thermal performance. However, the moisture content of exterior systems may be controlled by the use of an adequately water protective paint or coating [37], and this could also be stated in the technical sheets.

5.3.4. Differences between declared and measured properties

Relevant differences were found between declared and measured properties of lime-cork mortars (A1, A2), especially in terms of thermal conductivity, which ranged from 60% higher to more than twice the declared value. The increase observed is considered to be the result of the following circumstances:

- the lack of efficacy of the air-entraining admixtures, which resulted in reduced porosity in the tested materials. Indeed, thermal mortars A1 and A2 were found to have less than half of the declared open porosity. This reduction is concerning because the materials were carefully prepared following the manufacturer's instructions. Thus, if this low porosity was obtained in the laboratory, it is very likely to re-present itself when the materials are prepared in-situ, with presumably much less attention and time given to the preparation;
- the application of mortars by spatula. Thermal mortars are sensitive to manipulation, and it is expected that they provide better performance when applied by mechanical spraying. It is indeed expected that spray application does improve the entrance of air into the fresh mortar, resulting in higher porosity and, consequently, lower thermal conductivity of the hardened materials. A high amount of entrained air may also reduce the capillary water absorption [35], as large voids (above capillary range) work as water barriers. If strong differences are systematically found between the properties of thermal mortars applied by mechanical spraying and by spatula, it would be useful to provide some correlated indications in the technical sheets of the materials, when they are designed to be applied with both techniques.

6. Conclusions

The experimental campaign provided an extensive hygrothermal characterization of a selection of thermal mortars and thermal mortar-based insulation systems, useful as a numerical database for forthcoming numerical hygrothermal simulations. The thermal conductivity obtained in the experimental campaign was higher than designed by the manufactures in the case of all the thermal mortars analysed, probably due to the variability introduced by the application conditions. Nonetheless, all solutions appeared to be potentially beneficial for application in moderately cold climates (measured $\lambda \leq 0.20$ W/m.K). Furthermore, a strong dependency was observed in the thermal conductivity of thermal mortars on water content, $\lambda(w)$.

Experimental results showed that the use of standard samples of thermal mortars can lead to much higher water absorption coefficients than layered samples, as up to 75% higher A_w coefficients were observed. Moreover, the permeability to water vapour of the paints was found to vary noticeably depending if samples of single materials or complete systems were adopted. In particular, the s_d of paint C2 was found to be 4-times higher in the latter scenario, at dry conditions. These outcomes showed that the effect of layered constructions and interfacial phenomena can have a relevant influence on the hygric behaviour of complete systems. Thus, testing single materials only, which is the standard requirement for thermal mortar-based systems (EN 998-1), is in fact not sufficient for understanding the behaviour of composite insulation solutions based on thermal mortars.

For this reason, it would be beneficial to introduce some information concerning the hygric behaviour of complete systems into the technical documentation of thermal mortar-based insulation solutions. This additional data would help designers to better forecast the impact of thermal plastering and rendering systems on the moisture dynamics of walls, which is extremely important when dealing with historic constructions.

CRediT authorship contribution statement

Magda Posani: Investigation, Conceptualization, Visualization, Writing – original draft. **Rosário Veiga:** Supervision, Writing – review & editing. **Vasco Peixoto de Freitas:** Writing – review & editing.

Declaration of Competing Interest

The authors declare that they have no known competing financial interests or personal relationships that could have appeared to influence the work reported in this paper.

Acknowledgements

The authors thank the funding provided by FCT - Fundação para a Ciência e a Tecnologia [PD/BD/135192/2017], CONSTRUCT (LFC—Laboratory of Building Physics) - Research Unit Institute of R&D in Structures and Construction at FEUP (Faculty of Engineering of the University of Porto) and Project PRESERVE – Preservation of renders of built cultural heritage at LNEC (National Laboratory for Civil Engineering).

References

[1] S. Balibar, Energy transitions after COP21 and 22, C. R. Phys. 18 (2017) 479–487, https://doi.org/10.1016/J.CRHY.2017.10.003.
[2] A. Jordan, D. Huitema, H. Van Asselt, T. Rayner, and F. Berkhout, *Climate change policy in the European Union: Confronting the dilemmas of mitigation and adaptation?* Cambridge, UK, 2010. https://doi.org/10.1017/CBO9781139042772.
[3] European Commission, "2050 long-term strategy." [Online]. Available: https://ec.europa.eu/clima/policies/strategies/2050_en. [Accessed: 17-Jan-2020].
[4] European Commission, "Going climate-neutral by 2050: A strategic long-term vision for a prosperous, modern, competitive and climate-neutral EU economy", 2019. https://doi.org/10.2834/02074.
[5] M. Posani, R. Veiga, V.P. de Freitas, K. Kompatscher, H. Schellen, Dynamic hygrothermal models for monumental, historic buildings with HVAC systems: complexity shown through a case study, in *E3S Web Conf.*, 2020, vol. 172, p. 15007.
[6] A. Martínez-Molina, I. Tort-Ausina, S. Cho, J.L. Vivancos, Energy efficiency and thermal comfort in historic buildings: A review, Renew. Sustain. Energy Rev. 61 (2016) 70–85, https://doi.org/10.1016/j.rser.2016.03.018.
[7] European Project 3ENCULT – Efficient Energy for EU Cultural Heritage, 201-2014. [Online]. Available: http://www.3encult.eu/en/project/welcome/default.html. [Accessed: 11-Feb-2019].
[8] European Project "COOL Bricks – Climate Change, Cultural Heritage & Energy Efficient Monuments" ,2007-2013. [Online]. Available: http://www.co2olbricks.eu/index.php?id=43. [Accessed: 11-Feb-2019].
[9] European Project "EFFESUS– Energy Efficiency for EU Historic Districts Sustainability, 2016. [Online]. Available: http://www.effesus.eu/. [Accessed: 11-Feb-2019].
[10] V. Pracchi, A. Buda, Potentialities and criticalities of different retrofit guidelines in their application on different case studies, in: *The 3rd International Conference on Energy Efficiency in Historic Buildings (EEHB2018), Visby, Sweden, September 26th to 27th, 2018.*, 2018, pp. 283–293.
[11] A. Troi and Z. Bastian, Building Energy Efficiency Solutions: A handbook. Chapter 2.3: Cultural Heritage, in *Birkhauser*, 2015. https://doi.org/10.1017/CBO9781107415324.004.
[12] G. Carbonara, Energy efficiency as a protection tool, Energy Build. 95 (2015) 9–12, https://doi.org/10.1016/j.enbuild.2014.12.052.
[13] Council of Europe, "The Declaration of Amsterdam", *Directorate of Press and Information of the Council of Europe:* Strasburg, France, 1975. [Online]. Available: https://www.icomos.org/en/and/169-the-declaration-of-amsterdam [Accessed: 1 June 2021].
[14] M. Posani, R. Veiga, V. P. De Freitas, Historic buildings resilience: A view over envelope energy retrofit possibilities, in: The 8th International Conference on Building Resilience (ICBR2018), Lisbon, Portugal, November 14-16, 2018.
[15] D. Del Curto, V. Cinieri, Aerogel-based plasters and energy efficiency of historic buildings. Literature review and guidelines for manufacturing specimens destined for thermal tests, Sustainability (Switzerland) (2020), https://doi.org/10.3390/su12229457.
[16] ICOMOS. The Burra Charter (The Australia ICOMOS Charter for Places of Cultural Significance); Australia ICOMOS: Burwood, Australia, 2013. https://doi.org/10.1007/978-1-4419-0465-2_1046.
[17] M. Ganobjak, S. Brunner, J. Wernery, Aerogel materials for heritage buildings: Materials, properties and case studies, J. Cult. Herit. (2019), https://doi.org/10.1016/j.culher.2019.09.007.
[18] M. Posani, R. Veiga, V.P. de Freitas, Retrofitting historic walls: feasibility of thermal insulation and suitability of thermal mortars, Heritage 4 (3) (2021) 2009–2022, https://doi.org/10.3390/heritage4030114.
[19] M. Guizzardi, D. Derome, R. Vonbank, J. Carmeliet, Hygrothermal behavior of a massive wall with interior insulation during wetting, Build. Environ. (2015), https://doi.org/10.1016/j.buildenv.2015.01.034.
[20] European Committee for Standardization, EN 998-1:2017 - 'Specification for mortar for masonry - Part 1: Rendering and plastering mortar. *British Standards Institution*, 2017.
[21] A. Henry, J. Stewart, Practical building conservation: mortars, renders & plasters, English Heritage (2011), https://doi.org/10.1080/13556207.2014.858292.
[22] A. Ranesi, R. Veiga, P. Faria, Laboratory characterization of relative humidity dependent properties for plasters: A systematic review, Constr. Build. Mater. 304 (2021), 124595, https://doi.org/10.1016/j.conbuildmat.2021.124595.
[23] J. Maia, N.M.M. Ramos, R. Veiga, Evaluation of the hygrothermal properties of thermal rendering systems, Build. Environ. (2018), https://doi.org/10.1016/j.buildenv.2018.08.055.
[24] M.G. Gomes, I. Flores-Colen, H. Melo, A. Soares, Physical performance of industrial and EPS and cork experimental thermal insulation renders, Constr. Build. Mater. 198 (2019) 786–795, https://doi.org/10.1016/j.conbuildmat.2018.11.151.
[25] A. Brás, F. Gonçalves, P. Faustino, Cork-based mortars for thermal bridges correction in a dwelling: Thermal performance and cost evaluation, Energy Build. 72 (2014), https://doi.org/10.1016/j.enbuild.2013.12.022.
[26] J. Maia, N. M. M. Ramos, and R. Veiga, Assessment of test methods for the durability of thermal mortars exposure to freezing, *Mater. Struct. Constr.*, vol. 52, no. 6, 2019. https://doi.org/10.1617/s11527-019-1411-4.
[27] B. Mazhoud, F. Collet, S. Pretot, J. Chamoin, Hygric and thermal properties of hemp-lime plasters, Build. Environ. 96 (2016) 206–216, https://doi.org/10.1016/j.buildenv.2015.11.013.
[28] A. Arizzi, G. Cultrone, Aerial lime-based mortars blended with a pozzolanic additive and different admixtures: A mineralogical, textural and physical-mechanical study, Constr. Build. Mater. 31 (2012), https://doi.org/10.1016/j.conbuildmat.2011.12.069.
[29] R.H. Nosrati, U. Berardi, Hygrothermal characteristics of aerogel-enhanced insulating materials under different humidity and temperature conditions, Energy Build. (2018), https://doi.org/10.1016/j.enbuild.2017.09.079.
[30] J. Maia, et al., Hygrothermal performance of a new thermal aerogel-based render under distinct climatic conditions, Energy Build. 243 (2021), https://doi.org/10.1016/j.enbuild.2021.111001.
[31] M.L. Torres, P.A. García-Ruiz, Lightweight pozzolanic materials used in mortars: Evaluation of their influence on density, mechanical strength and water absorption, *Cem. Concr. Compos.*, 31(2), 2009. https://doi.org/10.1016/j.cemconcomp.2008.11.003.
[32] M. Behera, S. K. Bhattacharyya, A.K. Minocha, R. Deoliya, S. Maiti, Recycled aggregate from C&D waste & its use in concrete - A breakthrough towards sustainability in construction sector: A review, *Constr. Build. Mater.*, 68. 2014. https://doi.org/10.1016/j.conbuildmat.2014.07.003.
[33] E. Cintura, L. Nunes, B. Esteves, P. Faria, Agro-industrial wastes as building insulation materials: A review and challenges for Euro-Mediterranean countries, Ind. Crop. Prod. 171 (2021), 113833, https://doi.org/10.1016/j.indcrop.2021.113833.
[34] F. Barreca, C.R. Fichera, Use of olive stone as an additive in cement lime mortar to improve thermal insulation, Energy Build. 62 (2013), https://doi.org/10.1016/j.enbuild.2013.03.040.
[35] V. Corinaldesi, J. Donnini, A. Nardinocchi, Lightweight plasters containing plastic waste for sustainable and energy-efficient building, Constr. Build. Mater. 94 (2015), https://doi.org/10.1016/j.conbuildmat.2015.07.069.
[36] R. Walker, S. Pavía, Thermal performance of a selection of insulation materials suitable for historic buildings, Build. Environ. 94 (P1) (2015) 155–165, https://doi.org/10.1016/j.buildenv.2015.07.033.
[37] L. Coppola, D. Coffetti, E. Crotti, A. Marini, C. Passoni, T. Pastore, Lightweight cement-free alkali-activated slag plaster for the structural retrofit and energy upgrading of poor quality masonry walls, Cem. Concr. Compos. 104 (2019), https://doi.org/10.1016/j.cemconcomp.2019.103341.
[38] M. Vyšvařil, et al., Non-hydrophobized perlite renders for repair and thermal insulation purposes: Influence of different binders on their properties and durability, Constr. Build. Mater. 263 (2020), https://doi.org/10.1016/j.conbuildmat.2020.120617.
[39] Y. Govaerts, et al., Performance of a lime-based insulating render for heritage buildings, Constr. Build. Mater. 159 (2018) 376–389, https://doi.org/10.1016/j.conbuildmat.2017.10.115.
[40] F. Ascione, N. Cheche, R.F. De Masi, F. Minichiello, G.P. Vanoli, Design the refurbishment of historic buildings with the cost-optimal methodology: The case study of a XV European century Italian building, Energy Build. 99 (2015) 162–176, https://doi.org/10.1016/j.enbuild.2015.04.027.
[41] C. Cornaro, V.A. Puggioni, R.M. Strollo, Dynamic simulation and on-site measurements for energy retrofit of complex historic buildings: Villa Mondragone case study, J. Build. Eng. 6 (2016) 17–28, https://doi.org/10.1016/j.jobe.2016.02.001.
[42] G.B.A. Coelho, H. Entradas Silva, F.M.A. Henriques, Impact of climate change in cultural heritage: from energy consumption to artefacts' conservation and building rehabilitation, Energy Build. (2020), https://doi.org/10.1016/j.enbuild.2020.110250.
[43] F. Ascione, N. Bianco, R. F. De Masi, F. De'Rossi, G. P. Vanoli, Energy retrofit of an educational building in the ancient center of Benevento. Feasibility study of energy savings and respect of the historical value, *Energy Build.*, 95, 2015, 72–183. https://doi.org/10.1016/j.enbuild.2014.10.072.
[44] S. Cirami, G. Evola, A. Gagliano, G. Margani, Thermal and economic analysis of renovation strategies for a historic building in mediterranean area, Buildings 7 (3) (2017) 60, https://doi.org/10.3390/buildings7030060.
[45] R. Agliata, A. Marino, L. Mollo, P. Pariso, Historic building energy audit and retrofit simulation with hemp-lime plaster-A case study, *Sustain.*, 12(11), 2020. https://doi.org/10.3390/su12114620.
[46] European Organisation for Technical Approvals (EOTA). ETAG 004—Guideline for European Technical Approval of External Thermal Insulation Composite Systems (ETICS) with Rendering; *EOTA:* Brussels, Belgium, 2013.

[47] M. Posani, R. Veiga, V.P. de Freitas, Towards resilience and sustainability for historic buildings: A review of envelope retrofit possibilities and a discussion on hygric compatibility of thermal insulations, Int. J. Archit. Herit. (2019), https://doi.org/10.1080/15583058.2019.1650133.

[48] European Committee for Standardization (CEN), EN 1015-11:2019 - Methods of test for mortar for masonry - Part 11: Determination of flexural and compressive strength of hardened mortar. *British Standards Institution*, 2019.

[49] European Committee for Standardization (CEN), EN 1015-19:2008 - Methods of test for mortar for masonry - Part 19: Determination of water vapour permeability of hardened rendering and plastering mortars. *British Standards Institution*, 2008.

[50] R. Veiga, A. Fragata, A.L. Velosa, A.C. Magalhães, G. Margalha, Lime-based mortars: Viability for use as substitution renders in historical buildings, Int. J. Archit. Herit. 4 (2) (2010) 177–195, https://doi.org/10.1080/15583050902914678.

[51] R. Veiga, Air lime mortars: What else do we need to know to apply them in conservation and rehabilitation interventions? A review, Constr. Build. Mater. (2017), https://doi.org/10.1016/j.conbuildmat.2017.09.080.

[52] European Committee for Standardization (CEN), EN 1062-3:2008 - Paints and varnishes - Coating materials and coating systems for exterior masonry and concrete - Part 3. *British Standards Institution*, 2008.

[53] European Committee for Standardization (CEN), EN 1015-18:2002 - Methods of test for mortar for masonry - Part 18: Determination of water absorption coefficient due to capillary action of hardened mortar. *British Standards Institution*, 2002.

[54] European Committee for Standardization (CEN), EN 1745:2020 - Masonry and masonry products. Methods for determining thermal properties. *British Standards Institution*, 2020.

[55] National Laboratory for Civil Engineering (LNEC), FE Pa 44 - 'Test for wall coverings - determination of open porosity and bulk and real density (in Portuguese: ficha de ensaio - revestimentos de paredes - determinação da porosidade aberta e das massas volúmica aparente e real)'. *LNEC*: Lisbon., 2015.

[56] International Organization for Standardization (ISO), ISO 12571:2013 - Hygrothermal performance of building materials and products — Determination of hygroscopic sorption properties. *British Standards Institution*, 2013.

[57] European Committee for Standardization (CEN), EN 15801:2009 - Conservation of cultural property - Test methods - Determination of water absorption by capillarity. *British Standards Institution*, 2009.

[58] American Society for Testing and Materials (ASTM), ASTM. D7984-16:2016 - 'Standard Test Method for Measurement of Thermal Effusivity of Fabrics Using a Modified Transient Plane Source (MTPS) Instrument. *ASTM Internationa*l, 2016.

[59] European Committee for Standardization (CEN), EN 15803:2009 - Conservation of cultural property. Test methods. Determination of water vapour permeability (δp). *British Standards Institution*, 2009.

[60] European Committee for Standardization (CEN), EN 1015-10:1999 - Methods of test for mortar for masonry. Determination of dry bulk density of hardened mortar. *British Standards Institution*, 1999.

[61] N. Yüksel, The review of some commonly used methods and techniques to measure the thermal conductivity of insulation materials, Insul. Mater. Context Sustain. (2016), https://doi.org/10.5772/64157.

[62] J. M. P. Q. Delgado, A. C. Azevedo, A. S. Guimarães, Chapter 2. Hygrothermal properties of the tested materials, in: *Drying Kinetics in Building Materials and Components: The Interface Influence*, Springer, 2019.

[63] M.G. Gomes, I. Flores-Colen, F. da Silva, M. Pedroso, Thermal conductivity measurement of thermal insulating mortars with EPS and silica aerogel by steady-state and transient methods, Constr. Build. Mater. (2018), https://doi.org/10.1016/j.conbuildmat.2018.03.162.

[64] M. Amorim, V.P. de Freitas, I. Torres, T. Kisilewicz, U. Berardi, The influence of moisture on the energy performance of retrofitted walls, MATEC Web Conf. (2020), https://doi.org/10.1051/matecconf/202032201035.

[65] M.G. Gomes, I. Flores-Colen, L.M. Manga, A. Soares, J. de Brito, The influence of moisture content on the thermal conductivity of external thermal mortars, Constr. Build. Mater. (2017), https://doi.org/10.1016/j.conbuildmat.2016.12.166.

[66] J.L. Parracha, et al., Performance parameters of ETICS: Correlating water resistance, bio-susceptibility and surface properties, Constr. Build. Mater. (2021), https://doi.org/10.1016/j.conbuildmat.2020.121956.

[67] K. Hansen, Sorption Isotherms: A Catalogue. Technical Report 162/86, Technical University of Denmar (DTU), 1986.

[68] J. Zhao, J. Grunewald, U. Ruisinger, S. Feng, Evaluation of capillary-active mineral insulation systems for interior retrofit solution, Build. Environ. 115 (2017) 215–227, https://doi.org/10.1016/j.buildenv.2017.01.004.

[69] H. M. Künzel, *Simultaneous Heat and Moisture Transport in Building Components One- and two-dimensional calculation using simple parameters.* 1995. https://doi.org/ISBN v.3-8167-4103-7.

[70] N.M.M. Ramos, J.M.P.Q. Delgado, V.P. De Freitas, Influence of finishing coatings on hygroscopic moisture buffering in building elements, Constr. Build. Mater. (2010), https://doi.org/10.1016/j.conbuildmat.2010.05.017.

[71] P. Narloch, W. Piątkiewicz, B. Pietruszka, The effect of cement addition on water vapour resistance factor of rammed earth, *Materials (Basel).*, vol. 14, no. 9, 2021. https://doi.org/10.3390/ma14092249.

[72] International Organization for Standardization (ISO), ISO 12572:2016 - Hygrothermal performance of building materials and products - Determination of water vapour transmission properties, *British Standards Institution*, 2016.

[73] J. Maia, N.M.M. Ramos, R. Veiga, Durability of Thermal Rendering and Plastering Systems, FEUP- Univerity of Porto, PhD thesis, 2019.

[74] A. Worch, The behaviour of vapour transfer on building material surfaces: the vapour transfer resistance, J. Therm. Envel. Build. Sci. 28 (2) (2004) 187–200, https://doi.org/10.1177/1097196304044398.

[75] R. Plagge, G. Scheffler, A. Nicolai, Experimental Methods to Derive Hygrothermal Material Functions for Numerical Simulation Tools, in: *Buildings X Conference*, Clearwater Beach FL, USA. December 2007.

[76] A. Sicakova, M. Draganovska, M. Kovac, Water absorption coefficient as a performance characteristic of building mixes containing fine particles of selected recycled materials, Procedia Eng. (2017), https://doi.org/10.1016/j.proeng.2017.04.287.

[77] O. Horma, M. Charai, A. Mezrhab, M. Karkri, Thermal characterization of cement-plaster-expanded polystyrene composites, in: *2020 5th International Conference on Renewable Energies for Developing Countries (REDEC)*, 2020, pp. 1–6.

[78] S. Bouzit, F. Merli, M. Sonebi, C. Buratti, M. Taha, Gypsum-plasters mixed with polystyrene balls for building insulation: Experimental characterization and energy performance, Constr. Build. Mater. 283 (2021), https://doi.org/10.1016/j.conbuildmat.2021.122625.

[79] European Committee for Standardization (CEN), EN 12524:2000 - Building materials and products. Hygrothermal properties. Tabulated design values. *British Standards Institution*, 2000.

[80] International Organization for Standardization (ISO), ISO 10456:2007 - 'Building materials and products — Hygrothermal properties — Tabulated design values and procedures for determining declared and design thermal values. *British Standards Institution*, 2007.

[81] R. Walker, S. Pavía, Thermal and hygric properties of insulation materials suitable for historic fabrics, in: *Proceedings of III International Congress on Construction and Building Research.*, 2015.

[82] H. Trechsel, Moisture Control in Buildings, ASTM International, 1994.

[83] I. Flores-Colen, L. Silva, J. De Brito, V.P. De Freitas, Drying index for in-service physical performance assessment of renders, Constr. Build. Mater. (2016), https://doi.org/10.1016/j.conbuildmat.2016.03.034.

[84] J. Šadauskiene, E. Monstvilas, V. Stankevičius, The impact of exterior finish vapour resistance on the moisture state of building walls, Technol. Econ. Dev. Econ. 13 (1) (2007) 73–82, https://doi.org/10.1080/13928619.2007.9637779.

[85] V. Brito, T.D. Gonçalves, P. Faria, Coatings applied on damp building substrates: performance and influence on moisture transport, J. coatings Technol. Res. 8 (4) (2011) 513–525, https://doi.org/10.1007/s11998-010-9319-5.

[86] European Committee for Standardization (CEN), EN 1062-1:2004 - Paints and varnishes - Coating materials and coating systems for exterior masonry and concrete - Part 1. *British Standards Institution*, 2004.

[87] M. Pedroso *et al.*, Characterisation of a multilayer external wall thermal insulation system. Application in a Mediterranean climate, *J. Build. Eng.*, 30, 2020. https://doi.org/10.1016/j.jobe.2020.101265.

[88] I. Torres, R. Veiga, V. Freitas, Influence of substrate characteristics on behavior of applied mortar, J. Mater. Civ. Eng. (2018), https://doi.org/10.1061/(asce)mt.1943-5533.0002339.

[89] M. Thomson, J. E. Lindqvist, J. Elsen, C. Groot, 2.5 Porosity of mortars, *Characterisation Old Mortars with Respect to their Repair-Final Rep. RILEM TC 167-COM*, pp. 77–106, 2004.

[90] D. Silveira, A. Gonçalves, I. Flores-Colen, R. Veiga, I. Torres, R. Travincas, Evaluation of in-service performance factors of renders based on in-situ testing techniques, *J. Build. Eng.*, 101806, 2020. https://doi.org/10.1016/j.jobe.2020.101806.

[91] J.M.P.Q. Delgado, V.P. de Freitas, A.S. Guimarães, Water movement in building walls: interfaces influence on the moisture flux, Heat Mass Transf. und Stoffuebertragung (2016), https://doi.org/10.1007/s00231-016-1755-z.

[92] A.S. Guimarães, J.M.P.Q. Delgado, A.C. Azevedo, V.P. de Freitas, Interface influence on moisture transport in buildings, Constr. Build. Mater. (2018), https://doi.org/10.1016/j.conbuildmat.2017.12.040.

[93] T.S. Freitas, A. S. Guimarães, S. Roels, V. P. de Freitas, A. Cataldo, Is the time-domain reflectometry (TDR) technique suitable for moisture content measurement in low-porosity building materials?, *Sustain.*, 12(19), 2020. https://doi.org/10.3390/SU12197855.

[94] Fraunhofer IBP (Fraunhofer Institute for Building Physics). WUFI Pro (version 5.3) [Computer software]. Stuttgart, Germany. Detailes Online, available: https://wufi.de/en/. [Accessed: 29-Mar-2018].

[95] M. Posani, R. Veiga, V. P. de Freitas, Thermal Retrofit for Histric Massive Walls in Temperate Climates: risks and opportunities, in *ENCORE 2020 – 4º Encontro de Conservação e Reabilitação de Edifícios, Lisboa,* 3-6 November 2020.

[96] European Committee for Standardization (CEN), EN 12664:2002 - Thermal performance of building materials and products. Determination of thermal resistance by means of guarded hot plate and heat flow meter methods. Dry and moist products of medium and low thermal resistance. *British Standards Institution*, 2002.